activated T cells in higher frequency as compared with tumor treated with AdRGD-CCL19 injection alone. These results correlate closely with differences in the antitumor effects (Figures 1 and 6), strongly suggesting that efficient accumulation of activated tumor-specific CTLs at a local tumor site is a key factor for establishment of efficacious cancer immunotherapy.

Discussion

Investigations of the relationship between the prognosis and the infiltration frequency of tumor-associated immune cells in patients with cancer have indicated that post-treatment recurrence or metastasis is significantly suppressed in cases that exhibit high immune cell-infiltration in primary tumor tissue,[34–36] and it is widely believed that T cells represent the most potent antitumor effector cells.[37–39] Therefore, the establishment of immunotherapy capable of promoting tumor cell–immune cell interaction is considered critical for improving the cure rate for cancer. Based on these results, an approach that attempts to reinforce immune cell accumulation in tumor tissue by applying chemokines, which control migration and infiltration of immune cells into the local site, is very attractive for the development of efficacious cancer immunotherapy. We previously demonstrated that tumor cells transduced with AdRGD encoding chemokine genes could produce and secrete chemokines that exhibit original bioactivity, and that inoculation with chemokine gene-transfected tumor cells was very useful for screening antitumor effects based on facilitation of chemokine secretion in tumor tissue.[25,26] In the present study, in order to evaluate the potential of chemokine-based immunogenetherapy for cancer by using an AdRGD system capable of efficient gene transduction in various tumors, we examined antitumor efficacy and accumulation of tumor-associated immune cells in mice directly injected with chemokine-expressing AdRGD into established tumor tissue.

An established murine B16BL6 melanoma injected with AdRGD-CCL17, -CCL19, -CCL20, -CCL21, -CCL22, -CCL27, -XCL1, or -CX3CL1 exhibited slightly delayed growth compared with control vector-injected tumor. Moreover, immunohistochemical analysis of these tumors demonstrated that intratumoral injection of AdRGD-CCL19 could significantly induce both $CD4^+$ and $CD8^+$ T-cell infiltration in parenchyma of tumor tissue, and that AdRGD-CCL17 injection was superior in promoting NK cell accumulation at the peritumoral site. Generally, the infiltration of immune cells rarely occurs in newly formed vessels in solid tumor, and immune cells that penetrate from existing blood vessels, which are present around tumor tissue, arrive at and accumulate in tumor parenchyma through the tumor border region.[40] This explains our observation that NK cells accumulated in the tumor peripheral zone, but did not infiltrate the tumor parenchyma upon intratumoral injection of chemokine-expressing AdRGD. On the other hand, we speculated that T-cell infiltration occurred directly from tumor vessels in the AdRGD-CCL19-treated group, because a large number of T cells were observed in the center of tumor tissue as well as near the border. This theory is supported by a previous report that CCL19 could increase the expression of cell adhesion molecules on vascular endothelial cells.[41] Although CCL19 and CCL21 are ligand for an identical chemokine receptor (CCR7), the level of T-cell infiltration in AdRGD-CCL21-injected tumors was obviously lower than that in AdRGD-CCL19-injected tumors. Similarly, regarding CCL17 and CCL22, which shared CCR4 as their receptor, the number of NK cells at periphery of AdRGD-CCL22-injected tumors was half of that of AdRGD-CCL17-injected tumors. Because chemokines are heparin/heparan sulfate-binding proteins and this property modulates their activity, diffusion, and stability in tissue, we speculated that an affinity to heparin/heparan sulfate of each chemokine might determine the difference of immune cell infiltration between CCL19- and CCL21-transduced tumors or between CCL17- and CCL22-transduced tumors. Previous studies have shown that intratumoral injections of CCL20 and CCL21 induce a large accumulation of mature DCs related with strong antitumor responses.[20,42] However, we did not detect significant increase of infiltrating $CD11c^+$ DCs in B16BL6 tumors injected with any chemokine-expressing AdRGDs including AdRGD-CCL20 and -CCL21. We speculated that the disagreement between our observation and the results in previous studies was caused by a difference of the tumor model which was examined. Therefore, in order to select appropriate chemokine for intratumoral gene transduction to augment tumor-infiltrating immune cells efficiently, we need to consider not only its receptor-specificity but also its *in vivo* characteristics and variety of tumors. However, we could not recognize a correlation between tumor suppressive effect and the number of tumor-infiltrating immune cells in mice treated with each chemokine-expressing AdRGD. Because most immune cells that infiltrated into tumors with injection of chemokine-expressing AdRGD were perforin-negative, that is, in naive status, combinational therapy that included another treatment, which could prime and activate immune effector cells, would be required for achievement of more potent antitumor efficacy.

We previously succeeded in efficiently transducing genes into DCs by applying the AdRGD system rather than a conventional vector,[28,43] and demonstrated that DCs transduced with the TAA gene using AdRGD are effective vaccine carriers that induce tumor-specific immune responses in mice.[33,44] Thus, we evaluated the antitumor effect in mice of intratumoral injection of chemokine-expressing AdRGD combined with intradermal immunization of DCs transduced with gp100 by AdRGD. Lytic activity of B16BL6-specific CTLs in splenocytes from B16BL6 tumor-bearing mice was considerably enhanced by single gp100/DC-immunization, indicating that administration of TAA/DCs could promote initiation and amplification of tumor immunity in individuals that exhibited ongoing tumor growth (ther-

apeutic protocol) as well as in intact mice (vaccine protocol). In combination with gp100/DC-immunization, intratumoral injection with AdRGD-CCL17, -CCL22, or -CCL27 markedly suppressed B16BL6 tumor growth in mice. In addition, immunohistochemical analysis and RT-PCR analysis using RNA isolated from treated tumors revealed that CCL17-, CCL22-, or CCL27-gene transduction induced efficient accumulation of activated T cells in tumor tissue. CCL19, on the other hand, only slightly induced activated T-cell accumulation in tumors of gp100/DC-immunized mice, whereas naive T cells were dramatically attracted to tumors injected with AdRGD-CCL19 alone. These conflicting results can be explained by the evidence that CCR7, which is the corresponding receptor for CCL19, is expressed on naive T cells, but not on effector-type T cells.[45] Kim *et al.* demonstrated that DC-stimulation led naive T cells to downregulation of lymphoid tissue homing related CCR7 and CXCR5, and upregulation of Th1/2 effector tissue-targeting chemoattractant receptors such as CCR4 (receptor for CCL17 and CCL22), CCR5, CXCR6, and CRTH2.[46] In addition, Mullins *et al.* reported that coexpression of CCR4 and CXCR3 by activated $CD8^+$ T cells derived from the peripheral blood or tumor-involved lymph nodes of patients with stage III metastatic melanoma was significantly associated with enhanced survival.[47] CCR10 (receptor for CCL27) is known as a chemokine receptor that is preferentially expressed among blood leukocytes by a subset of memory $CD4^+$ and $CD8^+$ T cells, and CCR10-positive T cells that coexpress the skin-homing receptor, cutaneous lymphocyte antigen, can act as both 'central' and 'effector' memory T cells.[48] These previous results supported our data that intratumoral injection of AdRGD-CCL17, -CCL22, or -CCL27, but not AdRGD-CCL19, was effective for promoting the anti-B16BL6 tumor efficacy and the infiltration of immune effector cells in mice immunized with gp100/DCs. Therefore, the selection of chemokine in cancer immunogenetherapy must consider the host's immune activation status and characteristics of other combined therapies on immunomodulation.

In conclusion, our results revealed that chemokine gene transduction into established tumors using AdRGD could enhance accumulation of immune cells, and would greatly contribute to the development of efficacious cancer immunogenetherapy based on 'Immune Cell Delivery System'. Additionally, combinational therapy that included immunization with TAA-delivered DCs and intratumoral injection of chemokine-expressing AdRGD, such as AdRGD-CCL17, -CCL22, and -CCL27, could more effectively suppress tumor growth as compared with each treatment alone, indicating that the combined treatment, which can systemically induce tumor-specific effector T cells, is a promising strategy for potentiating antitumor efficacy and tumor-infiltrating effector cells by direct injection of chemokine-expressing vector into tumors. Now, in order to apply our chemokine gene-based cancer immunotherapy to not only primary tumors but also metastatic tumors in which intratumoral injection of vectors is physically difficult, we are pushing forward development of transductionally and transcriptionally tumor-targeting vector, which can specifically deliver a chemokine gene into tumor cells by systemic administration.[49,50]

Abbreviations

AdRGD, RGD fiber-mutant adenoviral vector; CTL, cytotoxic T lymphocyte; DC, dendritic cell; FBS, fetal bovine serum; HE, hematoxylin and eosin; IFN, interferon; mAb, monoclonal antibody; NK, natural killer; PBS, phosphate-buffered saline; PFU, plaque-forming unit; RT-PCR, reverse transcription-polymerase chain reaction; TAA, tumor-associated antigen; Th, helper T cell.

Acknowledgements

We are grateful to Drs Osamu Yoshie and Takashi Nakayama (Department of Microbiology, Kinki University School of Medicine, Osaka-Sayama, Japan) for providing plasmids containing murine chemokine cDNA, to Yoshinobu Kimura (Department of Biopharmaceutics, Kyoto Pharmaceutical University, Kyoto, Japan) for technical assistance, and to KIRIN Brewery Co., Ltd (Tokyo, Japan) for providing recombinant murine granulocyte/macrophage colony-stimulating factor. The present study was supported in part by the Research on Health Sciences focusing on Drug Innovation from The Japan Health Sciences Foundation; by grants from the Bioventure Development Program of the Ministry of Education, Culture, Sports, Science and Technology of Japan, and by grants from the Ministry of Health, Labour and Welfare in Japan.

References

1 Urban JL, Schreiber H. Tumor antigens. *Annu Rev Immunol* 1992; **10**: 617–644.
2 Mackensen A, Carcelain G, Viel S, Raynal MC, Michalaki H, Triebel F *et al.* Direct evidence to support the immunosurveillance concept in a human regressive melanoma. *J Clin Invest* 1994; **93**: 1397–1402.
3 Smyth MJ, Godfrey DI, Trapani JA. A fresh look at tumor immunosurveillance and immunotherapy. *Nat Immunol* 2001; **2**: 293–299.
4 Tada T, Ohzeki S, Utsumi K, Takiuchi H, Muramatsu M, Li XF *et al.* Transforming growth factor-β-induced inhibition of T cell function. Susceptibility difference in T cells of various phenotypes and functions and its relevance to immunosuppression in the tumor-bearing state. *J Immunol* 1991; **146**: 1077–1082.
5 Ohm JE, Carbone DP. VEGF as a mediator of tumor-associated immunodeficiency. *Immunol Res* 2001; **23**: 263–272.
6 Jacobs SK, Wilson DJ, Kornblith PL, Grimm EA. Interleukin-2 or autologous lymphokine-activated killer cell treatment of malignant glioma: phase I trial. *Cancer Res* 1986; **46**: 2101–2104.

7 Rosenberg SA, Yannelli JR, Yang JC, Topalian SL, Schwartzentruber DJ, Weber JS *et al.* Treatment of patients with metastatic melanoma with autologous tumor-infiltrating lymphocytes and interleukin 2. *J Natl Cancer Inst* 1994; **86**: 1159–1166.
8 Mandelboim O, Vadai E, Fridkin M, Katz-Hillel A, Feldman M, Berke G *et al.* Regression of established murine carcinoma metastases following vaccination with tumour-associated antigen peptides. *Nat Med* 1995; **1**: 1179–1183.
9 Conry RM, Curiel DT, Strong TV, Moore SE, Allen KO, Barlow DL *et al.* Safety and immunogenicity of a DNA vaccine encoding carcinoembryonic antigen and hepatitis B surface antigen in colorectal carcinoma patients. *Clin Cancer Res* 2002; **8**: 2782–2787.
10 Dranoff G, Jaffee E, Lazenby A, Golumbek P, Levitsky H, Brose K *et al.* Vaccination with irradiated tumor cells engineered to secrete granulocyte-macrophage colony-stimulating factor stimulates potent, specific, and long-lasting anti-tumor immunity. *Proc Natl Acad Sci USA* 1993; **90**: 3539–3543.
11 Asada H, Kishida T, Hirai H, Satoh E, Ohashi S, Takeuchi M *et al.* Significant antitumor effects obtained by autologous tumor cell vaccine engineered to secrete interleukin (IL)-12 and IL-18 by means of the EBV/lipoplex. *Mol Ther* 2002; **5**: 609–616.
12 Mayordomo JI, Zorina T, Storkus WJ, Zitvogel L, Celluzzi C, Falo LD *et al.* Bone marrow-derived dendritic cells pulsed with synthetic tumour peptides elicit protective and therapeutic antitumour immunity. *Nat Med* 1995; **1**: 1297–1302.
13 Song W, Kong HL, Carpenter H, Torii H, Granstein R, Rafii S *et al.* Dendritic cells genetically modified with an adenovirus vector encoding the cDNA for a model antigen induce protective and therapeutic antitumor immunity. *J Exp Med* 1997; **186**: 1247–1256.
14 Nair SK, Heiser A, Boczkowski D, Majumdar A, Naoe M, Lebkowski JS *et al.* Induction of cytotoxic T cell responses and tumor immunity against unrelated tumors using telomerase reverse transcriptase RNA transfected dendritic cells. *Nat Med* 2000; **6**: 1011–1017.
15 Yoshie O, Imai T, Nomiyama H. Chemokines in immunity. *Adv Immunol* 2001; **78**: 57–110.
16 Zlotnik A, Yoshie O. Chemokines: a new classification system and their role in immunity. *Immunity* 2000; **12**: 121–127.
17 Murphy PM. The molecular biology of leukocyte chemoattractant receptors. *Annu Rev Immunol* 1994; **12**: 593–633.
18 Bokoch GM. Chemoattractant signaling and leukocyte activation. *Blood* 1995; **86**: 1649–1660.
19 Homey B, Muller A, Zlotnik A. Chemokines: agents for the immunotherapy of cancer? *Nat Rev Immunol* 2002; **2**: 175–184.
20 Sharma S, Stolina M, Luo J, Strieter RM, Burdick M, Zhu LX *et al.* Secondary lymphoid tissue chemokine mediates T cell-dependent antitumor responses *in vivo*. *J Immunol* 2000; **164**: 4558–4563.
21 Fushimi T, Kojima A, Moore MA, Crystal RG. Macrophage inflammatory protein 3α transgene attracts dendritic cells to established murine tumors and suppresses tumor growth. *J Clin Invest* 2000; **105**: 1383–1393.
22 Braun SE, Chen K, Foster RG, Kim CH, Hromas R, Kaplan MH *et al.* The CC chemokine CKβ-11/MIP-3β/ELC/Exodus 3 mediates tumor rejection of murine breast cancer cells through NK cells. *J Immunol* 2000; **164**: 4025–4031.
23 Miyata T, Yamamoto S, Sakamoto K, Morishita R, Kaneda Y. Novel immunotherapy for peritoneal dissemination of murine colon cancer with macrophage inflammatory protein-1β mediated by a tumor-specific vector, HVJ cationic liposomes. *Cancer Gene Ther* 2001; **8**: 852–860.
24 Guo J, Zhang M, Wang B, Yuan Z, Guo Z, Chen T *et al.* Fractalkine transgene induces T-cell-dependent antitumor immunity through chemoattraction and activation of dendritic cells. *Int J Cancer* 2003; **103**: 212–220.
25 Gao J-Q, Tsuda Y, Katayama K, Nakayama T, Hatanaka Y, Tani Y *et al.* Antitumor effect by interleukin-11 receptor α-locus chemokine/CCL27, introduced into tumor cells through a recombinant adenovirus vector. *Cancer Res* 2003; **63**: 4420–4425.
26 Okada N, Gao J-Q, Sasaki A, Niwa M, Okada Y, Nakayama T *et al.* Anti-tumor activity of chemokine is affected by both kinds of tumors and the activation state of the host's immune system: implications for chemokine-based cancer immunotherapy. *Biochem Biophys Res Commun* 2004; **317**: 68–76.
27 Mizuguchi H, Koizumi N, Hosono T, Utoguchi N, Watanabe Y, Kay MA *et al.* A simplified system for constructing recombinant adenoviral vectors containing heterologous peptides in the HI loop of their fiber knob. *Gene Therapy* 2001; **8**: 730–735.
28 Okada N, Masunaga Y, Okada Y, Iiyama S, Mori N, Tsuda T *et al.* Gene transduction efficiency and maturation status in mouse bone marrow-derived dendritic cells infected with conventional or RGD fiber-mutant adenovirus vectors. *Cancer Gene Ther* 2003; **10**: 421–431.
29 Mizuguchi H, Kay MA. Efficient construction of a recombinant adenovirus vector by an improved *in vitro* ligation method. *Hum Gene Ther* 1998; **9**: 2577–2583.
30 Mizuguchi H, Kay MA. A simple method for constructing E1- and E1/E4-deleted recombinant adenoviral vectors. *Hum Gene Ther* 1999; **10**: 2013–2017.
31 Lutz MB, Kukutsch N, Ogilvie AL, Rossner S, Koch F, Romani N *et al.* An advanced culture method for generating large quantities of highly pure dendritic cells from mouse bone marrow. *J Immunol Methods* 1999; **223**: 77–92.
32 Okada N, Tsujino M, Hagiwara Y, Tada A, Tamura Y, Mori K *et al.* Administration route-dependent vaccine efficiency of murine dendritic cells pulsed with antigens. *Br J Cancer* 2001; **84**: 1564–1570.
33 Okada N, Masunaga Y, Okada Y, Mizuguchi H, Iiyama S, Mori N *et al.* Dendritic cells transduced with gp100 gene by RGD fiber-mutant adenovirus vectors are highly efficacious in generating anti-B16BL6 melanoma immunity in mice. *Gene Therapy* 2003; **10**: 1891–1902.
34 Eerola AK, Soini Y, Paakko P. A high number of tumor-infiltrating lymphocytes are associated with a small tumor size, low tumor stage, and a favorable prognosis in operated small cell lung carcinoma. *Clin Cancer Res* 2000; **6**: 1875–1881.
35 Yin XY, Lu MD, Lai YR, Liang LJ, Huang JF. Prognostic significances of tumor-infiltrating S-100 positive dendritic cells and lymphocytes in patients with hepatocellular carcinoma. *Hepatogastroenterology* 2003; **50**: 1281–1284.
36 Fukunaga A, Miyamoto M, Cho Y, Murakami S, Kawarada Y, Oshikiri T *et al.* $CD8^+$ tumor-infiltrating lymphocytes together with $CD4^+$ tumor-infiltrating lymphocytes and dendritic cells improve the prognosis of patients with pancreatic adenocarcinoma. *Pancreas* 2004; **28**: e26–e31.
37 Naito Y, Saito K, Shiiba K, Ohuchi A, Saigenji K, Nagura H *et al.* $CD8^+$ T cells infiltrated within cancer cell nests as a prognostic factor in human colorectal cancer. *Cancer Res* 1998; **58**: 3491–3494.

38 Shankaran V, Ikeda H, Bruce AT, White JM, Swanson PE, Old LJ *et al.* IFN-γ and lymphocytes prevent primary tumour development and shape tumour immunogenicity. *Nature* 2001; **410**: 1107–1111.
39 Zhang L, Conejo-Garcia JR, Katsaros D, Gimotty PA, Massobrio M, Regnani G *et al.* Intratumoral T cells, recurrence, and survival in epithelial ovarian cancer. *N Engl J Med* 2003; **348**: 203–213.
40 Smolle J, Hofmann-Wellenhof R, Fink-Puches R. Melanoma and stroma: an interaction of biological and prognostic importance. *Semin Cutan Med Surg* 1996; **15**: 326–335.
41 Luther SA, Bidgol A, Hargreaves DC, Schmidt A, Xu Y, Paniyadi J *et al.* Differing activities of homeostatic chemokines CCL19, CCL21, and CXCL12 in lymphocyte and dendritic cell recruitment and lymphoid neogenesis. *J Immunol* 2002; **169**: 424–433.
42 Crittenden M, Gough M, Harrington K, Olivier K, Thompson J, Vile RG. Expression of inflammatory chemokines combined with local tumor destruction enhances tumor regression and long-term immunity. *Cancer Res* 2003; **63**: 5505–5512.
43 Okada N, Tsukada Y, Nakagawa S, Mizuguchi H, Mori K, Saito T *et al.* Efficient gene delivery into dendritic cells by fiber-mutant adenovirus vectors. *Biochem Biophys Res Commun* 2001; **282**: 173–179.
44 Okada N, Saito T, Masunaga Y, Tsukada Y, Nakagawa S, Mizuguchi H *et al.* Efficient antigen gene transduction using Arg-Gly-Asp fiber-mutant adenovirus vectors can potentiate antitumor vaccine efficacy and maturation of murine dendritic cells. *Cancer Res* 2001; **61**: 7913–7919.
45 Moser B, Loetscher P. Lymphocyte traffic control by chemokines. *Nat Immunol* 2001; **2**: 123–128.
46 Kim CH, Nagata K, Butcher EC. Dendritic cells support sequential reprogramming of chemoattractant receptor profiles during naive to effector T cell differentiation. *J Immunol* 2003; **171**: 152–158.
47 Mullins IM, Slingluff CL, Lee JK, Garbee CF, Shu J, Anderson SG *et al.* CXC chemokine receptor 3 expression by activated $CD8^+$ T cells is associated with survival in melanoma patients with stage III disease. *Cancer Res* 2004; **64**: 7697–7701.
48 Hudak S, Hagen M, Liu Y, Catron D, Oldham E, McEvoy LM *et al.* Immune surveillance and effector functions of $CCR10^+$ skin homing T cells. *J Immunol* 2002; **169**: 1189–1196.
49 Koizumi N, Mizuguchi H, Sakurai F, Yamaguchi T, Watanabe Y, Hayakawa T. Reduction of natural adenovirus tropism to mouse liver by fiber-shaft exchange in combination with both CAR- and αv integrin-binding ablation. *J Virol* 2003; **77**: 13062–13072.
50 Okada Y, Okada N, Mizuguchi H, Hayakawa T, Nakagawa S, Mayumi T. Transcriptional targeting of RGD fiber-mutant adenovirus vectors can improve the safety of suicide gene therapy for murine melanoma. *Cancer Gene Ther* 2005; **12**: 608–616.

HUMAN GENE THERAPY 17:264–279 (March 2006)

Modified Adenoviral Vectors Ablated for Coxsackievirus–Adenovirus Receptor, α_V Integrin, and Heparan Sulfate Binding Reduce *In Vivo* Tissue Transduction and Toxicity

NAOYA KOIZUMI,[1] KENJI KAWABATA,[1] FUMINORI SAKURAI,[1] YOSHITERU WATANABE,[2] TAKAO HAYAKAWA,[3] and HIROYUKI MIZUGUCHI[1,4]

ABSTRACT

Coxsackievirus and adenovirus receptor (CAR), α_V integrins, and heparan sulfate glycosaminoglycans (HSGs) are the tropism determinants of adenoviral (Ad) vectors *in vivo*. For the development of a targeted Ad vector, its broad tropism needs to be blocked (or reduced). We have previously developed Ad vectors with ablation of CAR, α_V integrin, and HSG binding by mutation of the FG loop in the fiber knob (deletion of T489, A490, Y491, and T492 of the fiber protein), deletion of the RGD motif of the penton base, and substitution of the fiber shaft domain for that derived from Ad type 35, respectively, and have shown that this triple-mutant Ad vector [Ad/ΔF(FG)ΔP-S35-L2] exhibits significantly lower transduction in mouse liver compared with the conventional Ad vector [Koizumi, N., Mizuguchi, H., Sakurai, F., Yamaguchi, T., Watanabe, Y., and Hayakawa, T. (2003). J. Virol. 77, 13062–13072]. In the present study, we optimized the fiber knob mutation for further reduced *in vivo* transduction and examined toxicity of the modified Ad vectors. Ad/ΔF(AB)ΔP-S35-L2, a triple-mutant Ad vector containing a mutation of the AB loop in the fiber knob (R412S, A415G, E416G, and K417G), mediated approximately 15,000- and 500-fold lower mouse liver transduction by intravenous and intraperitoneal administration, respectively, than the conventional Ad vector, and mediated 10-fold lower mouse liver transduction than did Ad/ΔF(FG)ΔP-S35-L2. Ad/ΔF(AB)ΔP-S35-L2 also exhibited lower transduction of other organs compared with Ad/ΔF(FG)ΔP-S35-L2 and the conventional Ad vector. Levels of both liver serum enzymes (aspartate transferase [AST] and alanine transferase (ALT)] and interleukin (IL)-6 in mouse serum after intravenous administration of Ad/ΔF(AB)ΔP-S35-L2 were similar to those in the nontreatment mouse serum, whereas the conventional Ad vector led to high levels of AST, ALT, and IL-6. We therefore succeeded in further improving the mutant Ad vector, abolishing both viral natural tropism and toxicity. This new Ad vector appears to be a fundamental vector for targeted gene delivery.

OVERVIEW SUMMARY

Nonspecific distribution of adenoviral (Ad) vectors in tissue after *in vivo* gene transfer is due to the relatively broad expression of coxsackievirus and adenovirus receptor (CAR) (the primary receptor), α_V integrin (the secondary receptor), and heparan sulfate (the tertiary receptor). Ad injection *in vivo* is associated with the initiation of the inflammatory response and tissue damage. In the present study, we have generated a modified Ad vector with ablation of CAR, α_V integrin, and heparan sulfate binding and examined toxicity (liver serum enzymes and interleukin-6) of the vector as well as its transduction properties. For CAR binding ablation, the AB or FG loop mutation of the fiber knob was employed, and gene transfer activity of the triple-mutant Ad vector containing the AB loop mutation was compared with that of the triple-mutant Ad vector containing the FG loop mutation and with that of the conventional Ad vector. The triple-mu-

[1]National Institute of Biomedical Innovation, Osaka 567-0085, Japan.
[2]Showa Pharmaceutical University, Tokyo 194-8543, Japan.
[3]Pharmaceuticals and Medical Devices Agency, Tokyo 100-0013, Japan.
[4]Graduate School of Pharmaceutical Sciences, Osaka University, Osaka 567-0871, Japan.

tant Ad vector containing the AB loop mutation was found to mediate significantly lower tissue transduction *in vivo*. Furthermore, this mutant Ad vector reduced (or blunted) liver toxicity and innate immunity responses (interleukin-6 production). Thus, the triple-mutant Ad vector will likely be a fundamental vector for targeted gene delivery.

INTRODUCTION

RECOMBINANT ADENOVIRAL (Ad) VECTORS are attractive vehicles for *in vitro* and *in vivo* gene transfer to a wide variety of cell types. This distribution is largely due to the relatively broad expression of the primary receptor, the coxsackievirus and adenovirus receptor (CAR), and the secondary receptor, α_v integrin, and the tertiary receptor, heparan sulfate glycosaminoglycans (HSGs). The lack of specificity limits the utility of Ad vectors in gene therapy. Targeted Ad vectors would improve not only the efficacy but also the safety profiles of the vectors by permitting the use of lower doses, which would be less toxic and potentially less immunogenic (Krasnykh *et al.*, 2000; Wickham, 2000; Mizuguchi and Hayakawa, 2004).

The initial phase of Ad infection involves at least two sequential steps. The first is attachment of the virus to the cell surface through binding of the knob domain of the fiber to CAR (Bergelson *et al.*, 1997; Tomko *et al.*, 1997). After attachment, interaction between the RGD motif of the penton bases with secondary host cell receptors, α_v integrins, facilitates internalization via receptor-mediated endocytosis (Wickham *et al.*, 1993, 1994). Furthermore, interaction between the KKTK (Lys-Lys-Thr-Lys) motif on the fiber shaft of Ad type 5 with HSGs and the length of the fiber shaft are involved in accumulation, in mouse and cynomolgus monkey liver, of systemically administered Ad vectors (Nakamura *et al.*, 2003; Smith *et al.*, 2003a,b; Vigne *et al.*, 2003).

Strategies to eliminate natural Ad tropism, based on modification of particular viral capsid proteins such as fiber and penton base (Wickham, 2000; Mizuguchi and Hayakawa, 2004), have been reported. To ablate CAR binding, Ad vectors containing an AB, DE, or FG loop mutation of the fiber knob (Bewley *et al.*, 1999; Kirby *et al.*, 1999; Alemany and Curiel, 2001; Einfeld *et al.*, 2001; Leissner *et al.*, 2001; Mizuguchi *et al.*, 2002; Smith *et al.*, 2002), Ad vectors containing the Ad type 40 short fiber (which has been hypothesized not to bind to any receptors; Nakamura *et al.*, 2003), and Ad vectors containing an external trimerization motif instead of the fiber knob (Hong *et al.*, 2003) have been developed. To ablate α_v integrin binding, Ad vectors with a deletion of the RGD (Arg-Gly-Asp) motif of the penton base (Einfeld *et al.*, 2001; Mizuguchi *et al.*, 2002; Vigne *et al.*, 2003) have been developed. To ablate HSG binding, Ad vectors mutated in the KKTK motif of the fiber shaft (Smith *et al.*, 2003b) have been developed.

Several groups have reported that Ad vectors from which CAR binding has been ablated do not change the biodistribution of Ad vectors (Alemany and Curiel, 2001; Leissner *et al.*, 2001; Mizuguchi *et al.*, 2002; Smith *et al.*, 2002), although Einfeld *et al.* have reported that CAR binding-ablated Ad vectors exhibit a 10-fold decrease in liver transduction (Einfeld *et al.*, 2001). Einfeld *et al.* have also reported that Ad vectors ablated for both CAR binding ablation and α_v integrin binding exhibit a more than 700-fold decrease in liver transduction (Einfeld *et al.*, 2001). Ad vectors ablated for α_v integrin binding, however, do not change their biodistribution (Mizuguchi *et al.*, 2002; Smith *et al.*, 2003b). Smith *et al.* have shown that HSG binding-ablated Ad vectors, in which the KKTK motif on the fiber shaft of Ad type 5 is changed to GAGA (Gly-Ala-Gly-Ala), exhibit a 15-fold decrease in liver transduction (Smith *et al.*, 2003b).

We have previously developed an Ad vector ablated for CAR, α_v integrin, and HSG binding by deleting four amino acids (T489, A490, Y491, and T492) from the FG loop of the fiber knob, deleting the RGD motif of the penton base, and substituting the fiber shaft domain for that derived from Ad type 35, which does not contain the HSG-binding motif (Koizumi *et al.*, 2003a). This triple-mutant Ad vector, on intravenous administration, showed more than 1000-fold lower gene transfer activity in mouse liver than the conventional Ad vector whereas double-mutant Ad vectors (ablated for CAR and α_v integrin binding, or for CAR and HSG binding), on intravenous administration, showed 100-fold lower gene transfer activity in mouse liver than the conventional Ad vector (Koizumi *et al.*, 2003a).

In the present study, we further improve the triple-mutant Ad vector by adding a mutation of the AB loop in the fiber knob (R412S, A415G, E416G, and K417G) instead of a deletion of the FG loop in the fiber knob. The AB loop in the fiber knob interacts directly with CAR and therefore must be the key anchor for the knob–CAR complex (Bewley *et al.*, 1999). In contrast, deletion of the FG loop in the fiber knob eliminates interactions between the fiber knob and CAR by changing the structure of the fiber knob (Kirby *et al.*, 1999). We examined in detail the gene transfer activity of the triple-mutant Ad vector containing a mutation of the AB loop in the fiber knob both *in vitro* and *in vivo* (intravenous and intraperitoneal administration) in comparison with the triple-mutant Ad vector containing a deletion of the FG loop in the fiber knob and the conventional Ad vector.

Another drawback of the Ad vector is the production (release) of cytokines and chemokines, as well as hepatotoxicity, after systemic injection of the vector (Lieber *et al.*, 1997; Liu *et al.*, 2003). The cytokines play a major causative role in liver damage associated with systemic Ad infusion as well as a role in the induction of an antiviral immune response. Cytokine production and release are thought to be the direct or indirect results of Ad uptake by Kupffer cells and their subsequent activation (Lieber *et al.*, 1997; Liu *et al.*, 2003) or lysis (Schiedner *et al.*, 2003). It is important to develop an Ad vector that reduces or blunts innate immune response. In the present study, we also show that systemic injection of the triple-mutant Ad vector does not increase serum interleukin (IL)-6 levels or liver serum enzymes (aspartate aminotransferase [AST] and alanine aminotransferase [ALT], which are hepatotoxicity marker enzymes).

MATERIALS AND METHODS

Cells

SK HEP-1 (endothelial cell line derived from human liver; Heffelfinger *et al.*, 1992) and 293 cells were cultured with Dulbecco's modified Eagle's medium (DMEM) supplemented with 10% fetal calf serum (FCS). Fiber-293 cells, which are stable transformants expressing Ad type 5 fiber protein (Koizumi *et al.*,

2003a), were cultured with DMEM supplemented with 10% FCS and hygromycin (GIBCO, 200 μg/ml; Invitrogen, Carlsbad, CA).

Plasmids and Ad vectors

The vector plasmid pAdHM59, which we used to generate Ad vectors containing a mutation of the AB loop of the fiber knob (R412S, A415G, E416G, and K417G), a deletion of the RGD motif in the penton base, and a substitution of the fiber shaft domain for that derived from Ad type 35, was constructed as follows. First, a polymerase chain reaction (PCR) fragment containing a sequence surrounding the AB loop of the Ad type 5 fiber knob gene (bp 32238–32495) was generated with primers (forward, 5′-ATTAATACTTTGTGGACCACACC-AGCTCCATCTCCTAACTGTAGcCTAAATGgAGgGggt-GATGCTAAACTCACTTTGGTCTTAACAAAA-3′ [the *Ase*I site is underlined and the mutation sequence is indicated by lower-case letters]; reverse, 5′-AGATCTCCATTTCTAAAG-TT-3′ [the *Bgl*II site is underlined]) and pGEM-Teasy-knob-CAR(+) as a template (Koizumi *et al.*, 2003a). The PCR fragment was then ligated with *Eco*RV-digested pcDNA3.1-Hygro (Invitrogen), resulting in pcDNA3.1-Hyg-AB4m. pcDNA3.1-Hyg-AB4mknob was constructed by three-piece ligation of (1) the *Afl*II/*Ase*I fragment of pF35-2.3(AseI) (Mizuguchi and Hayakawa, 2002), which contains the fiber shaft of Ad type 35, (2) the *Ase*I/*Bgl*II fragment of pcDNA3.1-Hyg-AB4m, and (3) the *Afl*II/*Bgl*II fragment of pcDNA3.1-Hygro. Next, pHM-S35-K5-AB4m was constructed by three-piece ligation of (1) the *Afl*II/*Bgl*II fragment of pcDNA3.1-Hyg-AB4mknob, (2) the *Mun*I/*Bgl*II fragment of pHM-S35-K5-CAR(+) (Koizumi *et al.*, 2003a), and (3) the *Afl*II/*Mun*I fragment of pHMCMV6 (Mizuguchi and Kay, 1999). pHM-S35-K5-AB4m contains the sequence encoding the CAR-binding ablated Ad type 5 fiber knob (mutation of the sequence encoding four amino acids in the AB loop), a *Csp*45I site in the HI loop, a *Cla*I site in the C-terminal end of the fiber knob-coding sequence, and the fiber shaft sequence of Ad type 35. pS35-K5-2.2-AB4m was then constructed by ligation of *Srf*I/*Mun*I-digested pHM14-Eco2 (Koizumi *et al.*, 2003b) and *Srf*I/*Mun*I-digested pHM-S35-K5-AB4m. Next, the *Srf*I/*Mun*I fragment of pS35-K5-2.2-AB4m was ligated with the *Srf*I/*Mun*I fragment of pHM14-Eco12, resulting in the creation of pHM14-Eco2-S35-AB4m, which contains the Ad genome from bp 27331 to the end of the Ad genome and contains the sequence encoding the substitution of the fiber shaft domain for that derived from Ad type 35 and the mutation of the AB loop of the fiber knob. Finally, pAdHM59 was constructed by ligation of *Eco*RI/*Cla*I-digested pHM14-Eco2-S35-AB4m (the location of the *Eco*RI site is bp 27332 in the Ad genome, whereas the *Cla*I site is in the C-terminal end of the fiber-coding sequence) and *Eco*RI/*Cla*I-digested pAdHM43 (Koizumi *et al.*, 2003a), which contains the complete Ad genome, deletion of the RGD motif in the penton base, and a *Cla*I site in the C-terminal end of the fiber-coding sequence. pAdHM59 has a complete E1/E3-deleted Ad genome with I-*Ceu*I, *Swa*I, and PI-*Sce*I sites in the E1 deletion region, *Pac*I sites at both ends of the Ad genome, and deletion of the RGD peptide-coding sequence of the penton base (MND-HAIRGDTFATRAE was changed to MNDTSRAE), and contains the chimeric fiber-coding sequence of the CAR binding-ablated Ad type 5 fiber knob (mutation of the AB loop-coding region of the fiber knob [R412S, A415G, E416G, and K417G]), the Ad type 35 fiber shaft sequences, and the Ad type 5 fiber tail sequence. pAdHM59 also contains a unique *Csp*45I site in the HI loop of the fiber knob-coding sequence and a *Cla*I site in the C-terminal end of the fiber knob-coding sequence. Therefore, the targeting ligands can be easily displayed in the fiber knob of the vectors by cloning the respective genes into these regions by simple *in vitro* ligation.

Ad vectors were constructed by an improved *in vitro* ligation method described previously (Mizuguchi and Kay, 1998, 1999). pAdHM59-CMVL2 and pAdHM54-CMVL2 were constructed by ligation of I-*Ceu*I/PI-*Sce*I-digested pAdHM59 and pAdHM54, respectively, and I-*Ceu*I/PI-*Sce*I-digested pCMVL1 (Mizuguchi and Kay, 1999). To construct pAdHM59-RGD-CMVL2, pAdHM59 was first digested with *Csp*45I and ligated with oligonucleotide 1 (5′-cggcctgtgactgccgcggagactgtttctgc-gatg-3′) and oligonucleotide 2 (5′-cgcatcgcagaaacagtctccgcg-gcagtcacaggc-3′), which corresponds to the RGD (RGD-4C) peptide, CDCRGDCFC, with high affinities for integrins ($\alpha_v\beta_3$ and $\alpha_v\beta_5$) (Koivunen *et al.*, 1995; Pasqualini *et al.*, 1997), resulting in the creation of pAdHM59-RGD. I-*Ceu*I/PI-*Sce*I-digested pAdHM59-RGD was then ligated with I-*Ceu*I/PI-*Sce*I-digested pCMVL1, resulting in the creation of pAdHM59-RGD-CMVL2.

To generate the virus, pAdHM59-CMVL2, pAdHM54-CMVL2, and pAdHM59-RGD-CMVL2 were digested with *Pac*I and purified by phenol–chloroform extraction and ethanol precipitation. Linearized DNAs were transfected into Fiber-293 cells (in the case of pAdHM54-CMVL2 and pAdHM59-CMVL2) or 293 cells (in the case of pAdHM59-RGD-CMVL2) with Super-Fect (Qiagen, Valencia, CA) according to the manufacturer's instructions. When pAdHM59-CMVL2 and pAdHM54-CMVL2 were transfected into normal 293 cells, the virus was not generated because the virus does not interact with 293 cellular receptors. Viruses [Ad/ΔF(AB)ΔP-S35-L2, Ad/ΔF(FG)ΔP-S35-L2, and Ad/ΔF(AB)ΔP-S35-RGD-L2] were prepared by standard methods with the exception that Ad/ΔF(AB)ΔP-S35-L2 and Ad/ΔF(FG)ΔP-S35-L2 were amplified with Fiber-293 cells, and that only the last step of viral amplification was performed by infection into normal 293 cells, as described previously (Koizumi *et al.*, 2003a). Ad/ΔF(FG)ΔP-S35-L2 is identical to Ad/ΔFΔP-S35-L2 in our previous report (Koizumi *et al.*, 2003a). A conventional luciferase-expressing Ad vector, Ad-L2, had been constructed previously (Mizuguchi and Kay, 1999). Viruses were purified by $CsCl_2$ step gradient ultracentrifugation followed by $CsCl_2$ linear gradient ultracentrifugation. Determination of virus particle titers was accomplished spectrophotometrically by the methods of Maizel *et al.* (1968). Virus particle titers of the vector stocks, prepared from five 150-mm dishes (approximately 8×10^7 cells), were as follows: Ad-L2, 1.8×10^{12} vector particles (VP)/ml; Ad/ΔF(AB)ΔP-S35-L2, 2.8×10^{12} VP/ml; Ad/ΔF(FG)ΔP-S35-L2, 3.3×10^{12} VP/ml; Ad/ΔF(AB)ΔP-S35-RGD-L2, 2.6×10^{12} VP/ml.

Western blotting

Five hundred nanograms of virus in 1× sample buffer containing 4% 2-mercaptoethanol was loaded onto a sodium dodecyl sulfate (SDS)–polyacrylamide gel after boiling for 5 min, followed by electrotransfer to a nitrocellulose membrane. After blocking in Block Ace (Dainippon Pharmaceutical, Osaka, Japan), the filters were incubated with a rabbit fiber knob polyclonal antibody (diluted 1:3000) (kindly provided by R.D. Gerard, University of

Texas Southwestern Medical Center, Dallas, TX), followed by incubation in the presence of peroxidase-labeled anti-rabbit antibody (diluted 1:10,000) (Cell Signaling Technology, Beverly, MA). The filters were developed by chemiluminescence (ECL Western blotting detection system; GE Healthcare, Little Chalfont, UK), and signals were read with an LAS-3000 imaging system (Fujifilm Medical Systems USA, Stamford, CT).

Adenovirus-mediated gene transduction into cultured cells

SK HEP-1 cells (1×10^4 cells) were seeded in a 96-well dish. On the next day, they were transduced with Ad-L2, Ad/ΔF(FG)ΔP-S35-L2, Ad/ΔF(AB)ΔP-S35-L2, or Ad/ΔF(AB)ΔP-S35-RGD-L2 (3000 VP/cell) for 1.5 hr. After a 48-hr culture period, luciferase production in the cells was measured with a luciferase assay system (PicaGene LT2.0 luminescence kit; Toyo Ink, Tokyo, Japan).

In the experiment to quantify Ad uptake into SK HEP-1 cells, the cells were incubated at 37°C for 1.5 hr with the corresponding virus, washed with phosphate-buffered saline (PBS), resuspended in 0.05% trypsin–0.5 m*M* EDTA-PBS solution, and incubated at 37°C for 10 min. After this incubation, the cells were incubated at 37°C for 10 min with 0.05% DNase I–0.5 *M* $MgCl_2$–PBS, washed with PBS, and resuspended in 0.1 *M* EDTA–PBS solution. Finally, the Ad genome DNA in the cells was quantified with a TaqMan fluorogenic detection system (ABI PRISM 7700 sequence detector; Applied Biosystems, Foster City, CA). Sample DNA was isolated with an automatic nucleic acid isolation system (NA-2000; Kurabo Industries, Osaka, Japan). The Ad vector DNA standard was pAdHM4 plasmid DNA (Mizuguchi and Kay, 1999). Primers for amplification were located in the E4 region, with the sequences CACCACCTCCCGGTACCATA (sense) and CCGCACCTGGTTTTGCTT (antisense). The fluorogenic detection probe had the sequence AACCTGCCCGCCGGCTATACACTG. Samples were amplified in 50 μl for 40 cycles in the ABI PRISM 7700 sequence detector with continuous fluorescence monitoring. Data were processed with ABI PRISM 7000 SD software (Applied Biosystems).

When SK HEP-1 cells were transfected with a complex of Ad/ΔF(AB)ΔP-S35-L2 and SuperFect (Qiagen), the cells (2×10^4 cells) were seeded in a 48-well dish. The next day, the cells were transduced with Ad/ΔF(AB)ΔP-S35-L2 (10,000 VP/cell) in the presence of SuperFect (0, 0.15, or 1.5 μg; Qiagen) for 1.5 hr. After a 48-hr culture period, luciferase production in the cells was measured with a luciferase assay system (PicaGene PGL5500; Toyo Ink).

In the competition experiments, SK HEP-1 cells (2×10^4 cells) were seeded in a 48-well dish. The next day, the cells were preincubated with RGD peptide (GRGDSP; TaKaRa, Osaka, Japan) (0, 40, or 200 μg/ml) for 10 min at room temperature. The cells were then transduced with Ad/ΔF(AB)ΔP-S35-RGD-L2 (300 VP/cell) for 0.5 hr. After 48 hr in culture, luciferase production in the cells was measured by luminescence assay (PicaGene LT2.0; Toyo Ink).

Adenovirus-mediated gene transduction in vivo

Ad-L2, Ad/ΔF(FG)ΔP-S35-L2, Ad/ΔF(AB)ΔP-S35-L2, or Ad/ΔF(AB)ΔP-S35-RGD-L2 was intravenously (3.0×10^{10} VP) or intraperitoneally (1.0×10^{11} VP) administered to C57BL/6 mice (male, 5 weeks old; obtained from Nippon SLC, Shizuoka, Japan). Forty-eight hours later, the heart, lung, liver, kidney, and spleen were isolated and homogenized as previously described (Xu *et al.*, 2001). Luciferase production was determined with a luciferase assay system (PicaGene 5500; Toyo Ink). Protein content was measured with a Bio-Rad assay kit (Bio-Rad, Hercules, CA), using bovine serum albumin as a standard.

The amounts of Ad genomic DNA in each organ were quantified with the TaqMan fluorogenic detection system (ABI PRISM 7700 sequence detector; Applied Biosystems). Samples were prepared with isolated DNA templates from each organ (25 ng) by the automatic nucleic acid isolation system (NA-2000; Kurabo Industries). The amounts of Ad DNA were quantified with the TaqMan fluorogenic detection system (Applied Biosystems), as described above.

Amounts of Ad vector DNA in liver parenchymal and nonparenchymal cells

Ad-L2, Ad/ΔF(FG)ΔP-S35-L2, or Ad/ΔF(AB)ΔP-S35-L2 was intravenously (3.0×10^{10} VP) or intraperitoneally (1.0×10^{11} VP) administered to C57BL/6 mice (male, 5 weeks old; Nippon SLC). Mice were anesthetized by intraperitoneal administration of pentobarbital sodium (Dainippon Pharmaceutical) 3 hr after Ad vector injection. Liver cells were separated into parenchymal cells (PCs; hepatocytes) and nonparenchymal cells (NPCs) (Kupffer cells and endothelial cells), as described previously (Nishikawa *et al.*, 1998). Briefly, the liver was perfused with HEPES buffer (pH 7.5) containing collagenase. The dispersed cells were separated into PC and NPC fractions by differential centrifugation. Quantitative PCR was performed to examine the amounts of Ad vector DNA in the PCs and NPCs. Total DNA, including the Ad vector DNA, was isolated from the PCs and NPCs by means of the automatic nucleic acid isolation system (NA-2000; Kurabo Industries). The amounts of Ad DNA were quantified with the TaqMan fluorogenic detection system (Applied Biosystems), as described above.

Blood clearance of Ad vectors

Blood samples were collected by retroorbital bleeding at the indicated times (2, 10, and 30 min; or 2, 60, 120, and 180 min) after intravenous (3.0×10^{10} VP) or intraperitoneal (1.0×10^{11} VP) administration of Ad-L2, Ad/ΔF(FG)ΔP-S35-L2, or Ad/ΔF(AB)ΔP-S35-L2. Total DNA, including the Ad vector DNA, was isolated from whole blood with a QIAamp DNA blood mini kit (Qiagen). The amounts of Ad DNA were quantified with the TaqMan fluorogenic detection system (Applied Biosystems), as described above.

Liver serum enzymes and interleukin-6 levels after systemic administration

Blood samples were collected from the inferior vena cava at the indicated times (3 or 48 hr) after intravenous (3.0×10^{11} VP) or intraperitoneal (1.0×10^{11} VP) administration of Ad-L2, Ad/ΔF(AB)ΔP-S35-L2 or Ad/ΔF(FG)ΔP-S35-L2. Serum samples were collected into separate tubes containing no anticoagulant for coagulation. The levels of AST and ALT in serum samples collected at 48 hr were measured with a Transaminase-CII kit (Wako Pure Chemical Industries, Osaka, Japan). IL-6 levels in serum samples collected 3 hr after Ad injection were

measured with an enzyme-linked immunosorbent assay (ELISA) kit (BioSource International, Camarillo, CA).

RESULTS

Construction of vectors that abolish natural viral tropism is the first step in the development of targeted Ad vectors. Identification and incorporation of a foreign ligand with high affinity for a specific cellular receptor into the capsid of Ad vectors that no longer infect cells would be the next step (Fig. 1A). This study was undertaken to improve a previously developed triple-mutant Ad vector that no longer infects cells by deletion of the FG loop of the fiber knob, deletion of the RGD motif of the penton base, and substitution of the fiber shaft domain with that derived from Ad type 35. Hepatocyte toxicity and innate immune response (IL-6 production) by systemic injection of the vectors were also examined.

Generation of several types of mutant Ad vector

To examine the effects of the various fiber knob mutations (mutation of AB loop or deletion of FG loop) in the triple-mutant Ad vector on gene transfer activity *in vitro* and *in vivo*, we constructed several types of mutant Ad vector expressing luciferase. Ad/ΔF(AB)ΔP-S35-L2 contains the Ad type 5 fiber knob

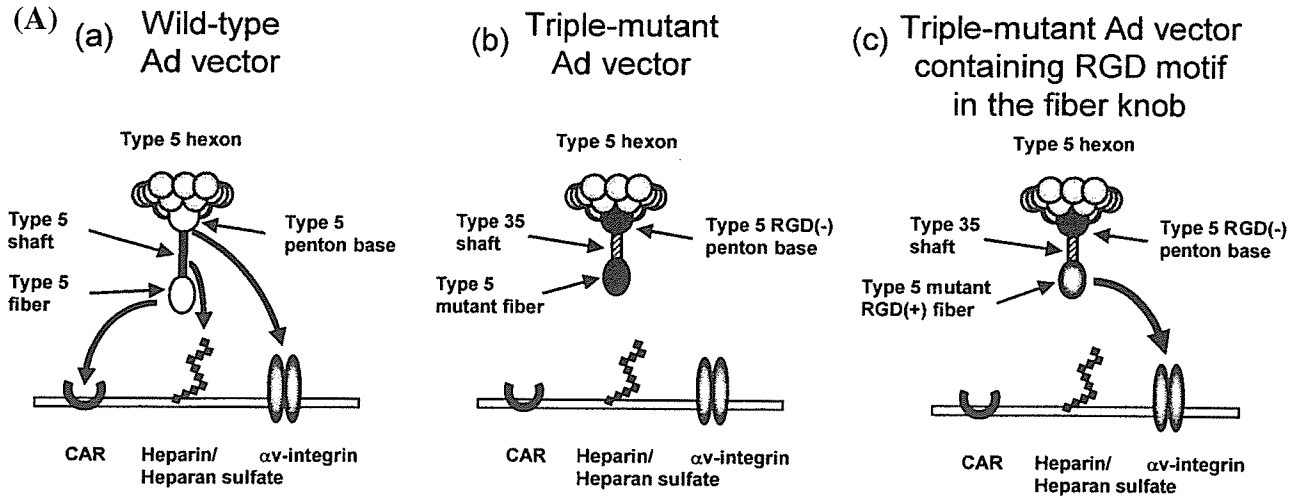

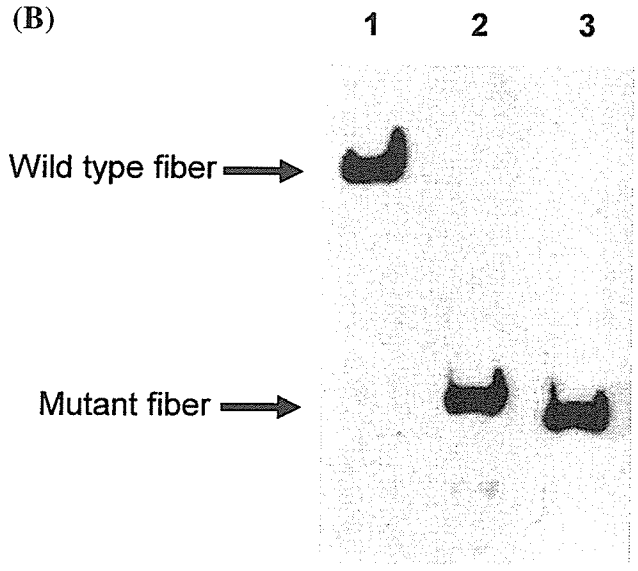

FIG. 1. Mutant Ad vectors. (**A**) Schematic diagram of the interaction of mutant Ad vectors with cells. The wild-type Ad vector infects cells by interactions of the fiber knob with CAR, the fiber shaft with HSGs, and the penton base with α_v integrin. The triple-mutant Ad vector does not have these interactions with cells. The triple-mutant Ad vector containing the RGD motif in the HI loop of the fiber knob infects cells via interaction of the RGD motif with α_v integrin. (**B**) Western blot analysis of the fiber protein in Ad-L2, Ad/ΔF(FG)ΔP-S35-L2, and Ad/ΔF(AB)ΔP-S35-L2. Five hundred nanograms of virus was separated on a 12% SDS–polyacrylamide gel, and the fiber protein was analyzed by Western blotting using a rabbit fiber knob polyclonal antibody as described in Materials and Methods. Lane 1, Ad-L2; lane 2, Ad/ΔF(FG)ΔP-S35-L2; lane 3, Ad/ΔF(AB)ΔP-S35-L2.

TABLE 1. ADENOVIRAL VECTOR MUTATIONS AND POTENTIAL CELL INTERACTIONS

Ad vector	*Amino acid sequence of knob domain*				*Type of Ad shaft*	*Type of Ad tail*	*Penton base*	*Type of Ad vector*[a]
	AB loop	*FG loop*	*HI loop*	*C terminus*				
Conventional Ad								
Ad-L2	–NCRLNAEKDA–	–TEGTAYTNAV–	–DTTPSA–	–QE stop	5 (22 β repeats)	5	MND–HAIRGDTFAT–RAE	a
Triple-mutant Ads								
Ad/ΔF(FG) ΔP-S35-L2	–NCRLNAEKDA–	–TEG----NAV– (Δa.a. 489–492)	–DTTSNPSA–	–QEID stop	35 (6 β repeats)	5	MND–TS----------RAE ΔRGD motif	b
Ad/ΔF(AB) ΔP-S35-L2	–NCSLNGGGDA– (4-a.a. mutation)	–TEGTAYTNAV–	–DTTSNPSA–	–QEID stop	35 (6 β repeats)	5	MND–TS----------RAE ΔRGD motif	b
Triple-mutant Ad containing RGD motif in fiber								
Ad/ΔF(AB) ΔP-S35-RGD-L2	–NCSLNGGGDA– (4-a.a. mutation)	–TEGTAYTNAV–	–DTTSACDCRG DCFCANPSA–	–QEID stop	35 (6 β repeats)	5	MND–TS----------RAE ΔRGD motif	c

[a]See Fig. 1A.

with a four-amino acid mutation of the AB loop (R412S, A415G, E416G, and K417G), the Ad type 35 fiber shaft, and a deletion of the RGD motif of the penton base. Ad/ΔF(FG)ΔP-S35-L2, which is identical to Ad/ΔFΔP-S35-L2 in our previous report (Koizumi *et al.*, 2003a), contains the Ad type 5 fiber knob with a four-amino acid deletion of the FG loop (T489, A490, Y491, and T492), the Ad type 35 fiber shaft, and deletion of the RGD motif of the penton base. Ad/ΔF(AB)ΔP-S35-RGD-L2 contains an RGD motif in the HI loop of the fiber knob in Ad/ΔF(AB)ΔP-S35-L2. Ad-L2 is a conventional Ad vector. All mutations of the mutant Ad vectors and possible interaction of each virus with the cells are summarized in Table 1 and Fig. 1A. All of the mutant Ad vectors used in this study were readily propagated with particle titers similar to that of the conventional Ad vector, Ad-L2 (see Materials and Methods).

To confirm the modification of the fiber protein in each Ad vector, Western blot analysis against fiber protein was performed with rabbit fiber knob polyclonal antibody (Fig. 1B). The mutant fiber and wild-type fiber are easily distinguished because the mutant fiber is smaller than the wild-type fiber because of the small size of the Ad type 35 fiber shaft and because Ad/ΔF(AB)ΔP-S35-L2 has a fiber protein four amino acids longer than that of Ad/ΔF(FG)ΔP-S35-L2. Western blot analysis shows the expected size of the fiber proteins, suggesting that each Ad vector should indeed contain the expected fiber protein.

Gene transfer in vitro

We examined the gene transfer activity in SK HEP-1 cells transduced with Ad/ΔF(AB)ΔP-S35-L2 in comparison with

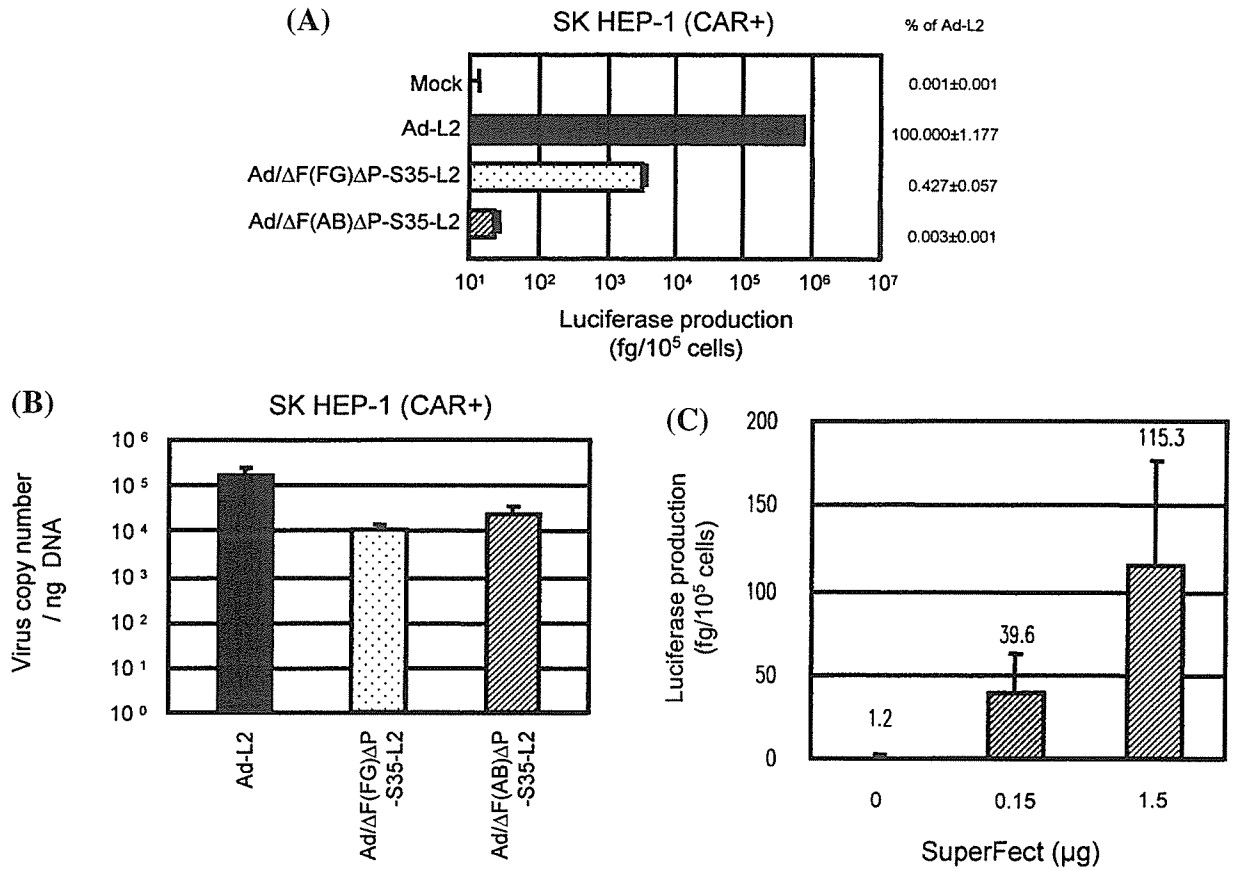

FIG. 2. Luciferase production and viral uptake in SK HEP-1 cells transduced with several Ad vectors. (**A**) Comparison of luciferase production in human cells transduced with Ad-L2, Ad/ΔF(FG)ΔP-S35-L2, or Ad/ΔF(AB)ΔP-S35-L2. SK HEP-1 cells were transduced with Ad-L2, Ad/ΔF(FG)ΔP-S35-L2, or Ad/ΔF(AB)ΔP-S35-L2 (3000 VP/cell) for 1.5 hr. After culture for 48 hr, luciferase production in the cells was measured by luminescence assay. Data are expressed as means ± SD (n = 4). Relative levels of luciferase expression are described by designating the value of Ad-L2 as 100. (**B**) Viral uptake in SK HEP-1 cells. SK HEP-1 cells were transduced with Ad-L2, Ad/ΔF(FG)ΔP-S35-L2, or Ad/ΔF(AB)ΔP-S35-L2 at 3000 VP/cell. After culture for 1.5 hr, the cells were washed with PBS, resuspended in 0.05% trypsin–0.5 m*M* EDTA–PBS solution, and incubated at 37°C for 10 min. After this incubation, the cells were incubated at 37°C for 10 min with 0.05% DNase I–0.5 *M* $MgCl_2$–PBS, washed with PBS, and resuspended in 0.1 *M* EDTA–PBS solution. The amounts of Ad genome DNA isolated from the cells were quantified with the TaqMan fluorogenic detection system. Data are expressed as means ± SD (n = 4). (**C**) Comparison of luciferase production in SK HEP-1 cells transduced with a complex of Ad/ΔF(AB)ΔP-S35-L2 and SuperFect. SK HEP-1 cells (2×10^4 cells) were seeded into a 24-well dish. The next day, the cells were either not transduced or were transduced with a complex of Ad/ΔF(AB)ΔP-S35-L2 and SuperFect (0.15 or 1.5 μg) (Qiagen) for 1.5 hr. After culture for 48 hr, luciferase production in the cells was measured with a luciferase assay system. Data are expressed as means ± SD (n = 4).

Ad/ΔF(FG)ΔP-S35-L2 or Ad-L2 (Fig. 2). SK HEP-1 cells express both CAR and α_v integrin (Koizumi *et al.*, 2001, 2003b). To measure the internalization of Ad particles into the cells, Ad genome DNA in the cells after 1.5 hr of transduction with each Ad vector was also quantified with the TaqMan fluorogenic detection system. Viral particles associated with the cellular surface were removed by trypsin–EDTA–PBS and DNase I–$MgCl_2$–PBS treatment as described in Materials and Methods. Cells transduced with Ad/ΔF(AB)ΔP-S35-L2 showed much lower luciferase production than those transduced with Ad/ΔF(FG)ΔP-S35-L2. Ad/ΔF(AB)ΔP-S35-L2 mediated only approximately 0.003% of the luciferase production of Ad-L2, whereas Ad/ΔF(FG)ΔP-S35-L2 mediated approximately 0.42% of that of Ad-L2 (Fig. 2A). In contrast, the amounts of Ad/ΔF(AB)ΔP-S35-L2 DNA and Ad/ΔF(FG)ΔP-S35-L2 DNA in SK HEP-1 cells were only 10-fold lower than those of Ad-L2 DNA. The amounts of Ad/ΔF(AB)ΔP-S35-L2 DNA in the cells were similar to those of Ad/ΔF(FG)ΔP-S35-L2 DNA (Fig. 2B).

Because Ad/ΔF(AB)ΔP-S35-L2 showed extremely low transduction activity, we examined luciferase production in SK HEP-1 cells transduced with Ad/ΔF(AB)ΔP-S35-L2 in the presence of SuperFect (polyamidoamine dendrimer reagent; Qiagen). Ad/ΔF(AB)ΔP-S35-L2 mediated high levels of luciferase production in a dose-dependent manner with SuperFect (Fig. 2C). Therefore, low luciferase production by Ad/ΔF(AB)ΔP-S35-L2 is likely due to a lack of specific binding activity between the virus and target cells and to endosomal escape, but it was not due to the virus being defective. These results suggest that the abolishment of CAR, integrin, and HSG binding of Ad vectors significantly reduces transduction efficiency and that the four-amino acid mutation of the AB loop of the fiber knob reduces transduction to a greater extent than does the four-amino acid deletion of the FG loop of the fiber knob.

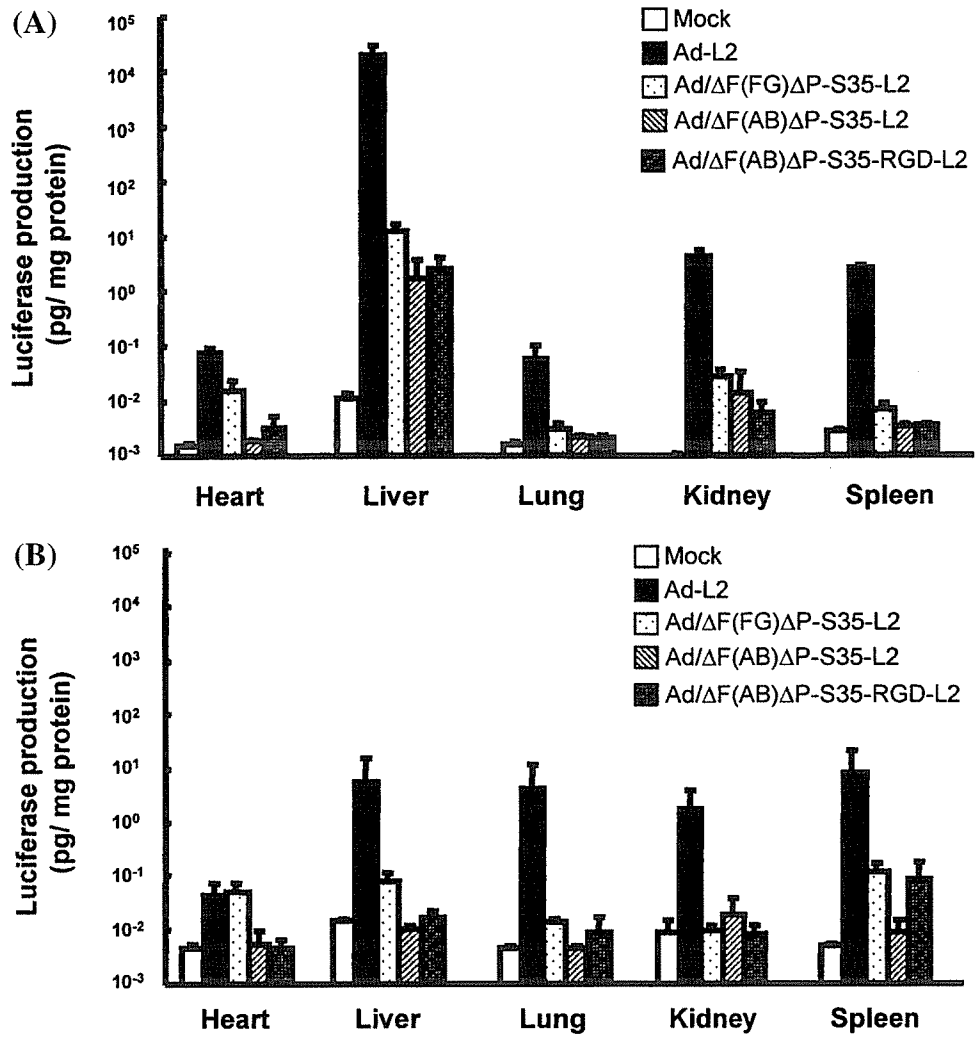

FIG. 3. Luciferase production in mice after systemic administration of Ad-L2, Ad/ΔF(FG)ΔP-S35-L2, or Ad/ΔF(AB)ΔP-S35-L2, or Ad/ΔF(AB)ΔP-S35-RGD-L2. Ad-L2, Ad/ΔF(FG)ΔP-S35-L2, Ad/ΔF(AB)ΔP-S35-L2, or Ad/ΔF(AB)ΔP-S35-RGD-L2 was (**A**) intravenously (3.0×10^{10} VP) or (**B**) intraperitoneally (1.0×10^{11} VP) injected into mice. Forty-eight hours later, the heart, lung, liver, kidney, and spleen were harvested and luciferase production was measured by a luciferase assay system. All data represent the means ± SD of four to six mice.

Gene transfer in vivo

Next, to examine whether natural Ad tropism to tissues, including liver, can be more suppressed by Ad/ΔF(AB)ΔP-S35-L2 in comparison with Ad/ΔF(FG)ΔP-S35-L2, each Ad vector was administered to mice by either intravenous (3.0×10^{10} VP) or intraperitoneal (1.0×10^{11} VP) injection, and luciferase production in the organ was measured (Figs. 3 and 4). In the case of intraperitoneal injection, a high dose of Ad vector (1.0×10^{11} VP) was injected because luciferase production was not detected in mouse tissue after intraperitoneal injection of 3.0×10^{10} VP of either Ad/ΔF(FG)ΔP-S35-L2 or Ad/ΔF(AB)ΔP-S35-L2. With intravenous injection, Ad/ΔF(AB)ΔP-S35-L2 mediated approximately 15,000-fold lower liver transduction than Ad-L2, and resulted in approximately 10-fold lower liver transduction compared with Ad/ΔF(FG)ΔP-S35-L2 (Fig. 3A). A similar pattern was observed in the heart, lung, kidney, and spleen, although the absolute levels of luciferase production were much lower compared with those in the liver.

With intraperitoneal injection, Ad-L2 mediated similar levels of luciferase production in the liver, lung, kidney, and spleen (Fig. 3B). The suppressive pattern of luciferase production in each organ after intraperitoneal injection of Ad/ΔF(AB)ΔP-S35-L2 and Ad/ΔF(FG)ΔP-S35-L2 was similar to that after intravenous injection. Ad/ΔF(AB)ΔP-S35-L2 showed much more reduced luciferase production in the organs than did Ad/ΔF(FG)ΔP-S35-L2 (Fig. 3B). Luciferase production in each organ after intraperitoneal injection of Ad/ΔF(AB)ΔP-S35-L2 was at almost background levels. These results indicate that the triple-mutant Ad vector containing a mutation of the AB loop of the fiber knob exhibits much lower luciferase production than does the triple-mutant Ad vector containing a mutation of the FG loop of the fiber knob, in both intravenously and intraperitoneally injected mice.

Distribution of Ad vectors after systemic administration

To examine the biodistribution of Ad/ΔF(AB)ΔP-S35-L2, Ad/ΔF(FG)ΔP-S35-L2, and Ad-L2 in mice at a early stage after intravenous (3×10^{10} VP) and intraperitoneal (1×10^{11} VP) injection, the amounts of Ad DNA in organs 3 hr after Ad vector injection were measured with the TaqMan fluorogenic detection system. The amounts of Ad DNA in organs after intravenous injection showed no significant difference among mice injected with Ad/ΔF(AB)ΔP-S35-L2, Ad/ΔF(FG)ΔP-S35-L2, or Ad-L2 (Fig. 4A), although the amounts of Ad/ΔF(AB)ΔP-S35-L2 and Ad/ΔF(FG)ΔP-S35-L2 in the kidney were less than that of Ad-L2. In the case of intraperitoneal injection, Ad/ΔF(AB)ΔP-S35-L2 and Ad/ΔF(FG)ΔP-S35-L2 showed higher or similar amounts of Ad DNA in the liver or spleen, respectively, than Ad-L2 (Fig. 4B).

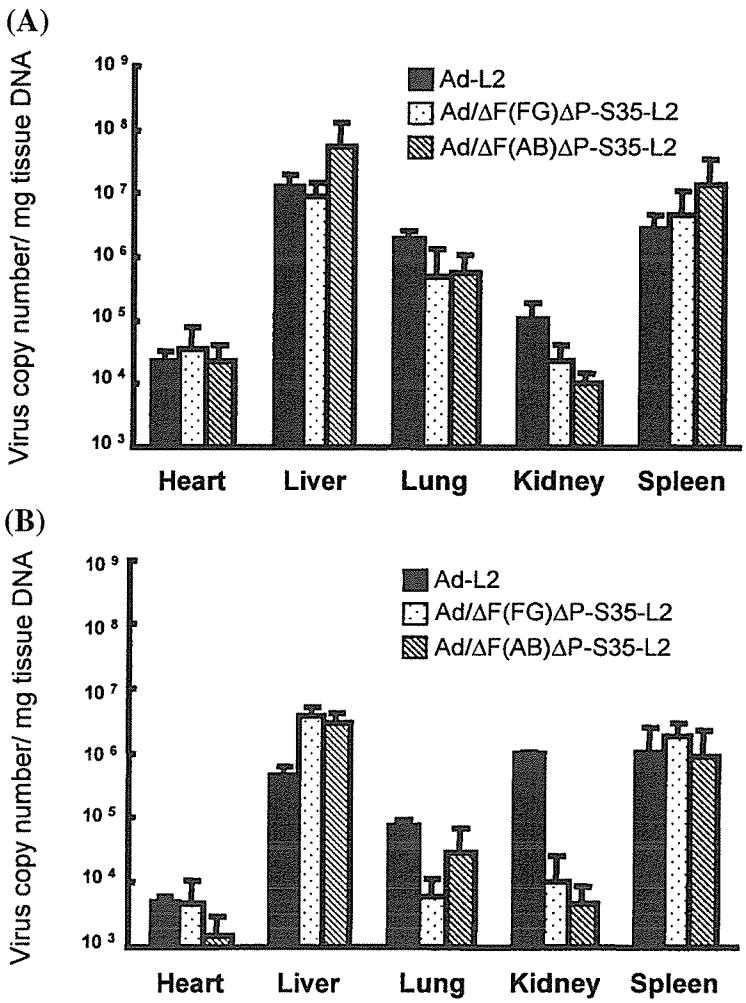

FIG. 4. Biodistribution of viral DNA after systemic administration of Ad-L2, Ad/ΔF(FG)ΔP-S35-L2, or Ad/ΔF(AB)ΔP-S35-L2 into mice. Ad-L2, Ad/ΔF(FG)ΔP-S35-L2, or Ad/ΔF(AB)ΔP-S35-L2 was (**A**) intravenously (3.0×10^{10} VP) or (**B**) intraperitoneally (1.0×10^{11} VP) injected into mice. Three hours later, the heart, lung, liver, kidney, and spleen were harvested and Ad vector DNA was measured with the quantitative TaqMan PCR assay. All data represent the means ± SD of four to six mice.

Less Ad/ΔF(AB)ΔP-S35-L2 accumulated in the heart, lung, and kidney compared with Ad-L2. The data regarding luciferase production (Fig. 3) and the amounts of Ad DNA in most organs, especially the liver (Fig. 4), showed discrepancies in the cases of both intravenous and intraperitoneal injection.

Amounts of Ad vector DNA in liver parenchymal and nonparenchymal cells

Next, to examine why there is an especially large difference between luciferase production and Ad DNA accumulation in the liver, the amounts of Ad/ΔF(AB)ΔP-S35-L2, Ad/ΔF(FG)ΔP-S35-L2, and Ad-L2 delivered to parenchymal cells (PCs; hepatocyte) and nonparenchymal cells (NPCs; Kupffer cells and endothelial cells) 3 hr after injection were measured with the TaqMan fluorogenic detection system (Fig. 5). In the case of intravenous injection of Ad vector at 3×10^{10} VP, more Ad-L2 DNA was found in PCs than in NPCs, whereas there was less Ad/ΔF(AB)ΔP-S35-L2 and Ad/ΔF(FG)ΔP-S35-L2 DNA in PCs than in NPCs (Fig. 5A). This finding is consistent with our previous reports based on analysis by semiquantitative PCR (Koizumi *et al.*, 2003a). In the case of intraperitoneal injection of Ad vector at 1×10^{11} VP, Ad/ΔF(AB)ΔP-S35-L2, Ad/ΔF(FG)ΔP-S35-L2, and Ad-L2 DNA accumulated more in NPCs than in PCs (Fig. 5B). Thus, lower luciferase production in the liver after intravenous and intraperitoneal injection of Ad/ΔF(AB)ΔP-S35-L2 and Ad/ΔF(FG)ΔP-S35-L2 would be partly due to higher accumulation of vectors in NPCs. The NPCs might take up Ad via phagocytosis and resolve viral DNA, resulting in lower gene expression.

Blood clearance of Ad vectors

To examine the biodistribution in more detail, the blood clearance rates of Ad/ΔF(AB)ΔP-S35-L2, Ad/ΔF(FG)ΔP-S35-L2, and Ad-L2 in mice were measured with the TaqMan fluorogenic detection system (Fig. 6). In the case of intravenous injection, blood clearance curves for Ad/ΔF(AB)ΔP-S35-L2, Ad/ΔF(FG)ΔP-S35-L2, and Ad-L2 were similar, and all the vectors showed rapid decrease from the bloodstream (Fig. 6A). In the case of intraperitoneal injection, Ad/ΔF(AB)ΔP-S35-L2 and Ad/ΔF(FG)ΔP-S35-L2 showed similar blood clearance curves. The amounts of Ad/ΔF(AB)ΔP-S35-L2 and Ad/ΔF(FG)ΔP-S35-L2 DNA were approximately 10-fold higher than those of Ad-L2 DNA between 60 and 120 min after injection (Fig. 6B). The area under the curve (AUC_{2-180}) values of Ad/ΔF(AB)ΔP-S35-L2 and Ad/ΔF(FG)ΔP-S35-L2 were 5- to 7-fold higher than that of Ad-L2 (data not shown). Higher levels of Ad/ΔF(AB)ΔP-S35-L2 and Ad/ΔF(FG)ΔP-S35-L2 were found to be introduced into the bloodstream from the intraperitoneum than Ad-L2.

Liver serum enzymes and serum interleukin-6 levels after administration of Ad vector

Systemic administration of Ad vectors results in the initiation of inflammation and strong innate immunity responses in animals and humans (Schnell *et al.*, 2001; Muruve, 2004), and this toxicity limits the utility of Ad vectors for gene therapy. To evaluate the toxicity of each Ad vector, we measured the levels of AST, ALT, and IL-6 in serum after systemic administration. After injection of Ad/ΔF(AB)ΔP-S35-L2 and Ad/ΔF(FG)ΔP-S35-L2 in mice (both by intravenous and intraperitoneal injection), the levels of AST and ALT in serum were similar to those in nontreated mice, suggesting that Ad/ΔF(AB)ΔP-S35-L2 and Ad/ΔF(FG)ΔP-S35-L2 did not show liver toxicity (Fig. 7). In contrast, Ad-L2 led to high levels of AST and ALT in serum after intravenous injection (Fig. 7A). In the case of IL-6, neither intravenous nor intraperitoneal injection of Ad/ΔF(AB)ΔP-S35-L2 or Ad/ΔF(FG)ΔP-S35-L2 mediated IL-6 production, whereas injection of Ad-L2 led to high levels of IL-6 in serum (Fig. 8). These results suggest that Ad/ΔF(AB)ΔP-S35-L2 and Ad/ΔF(FG)ΔP-S35-L2 show less liver toxicity and innate immunity reaction (IL-6 production) after systemic administration.

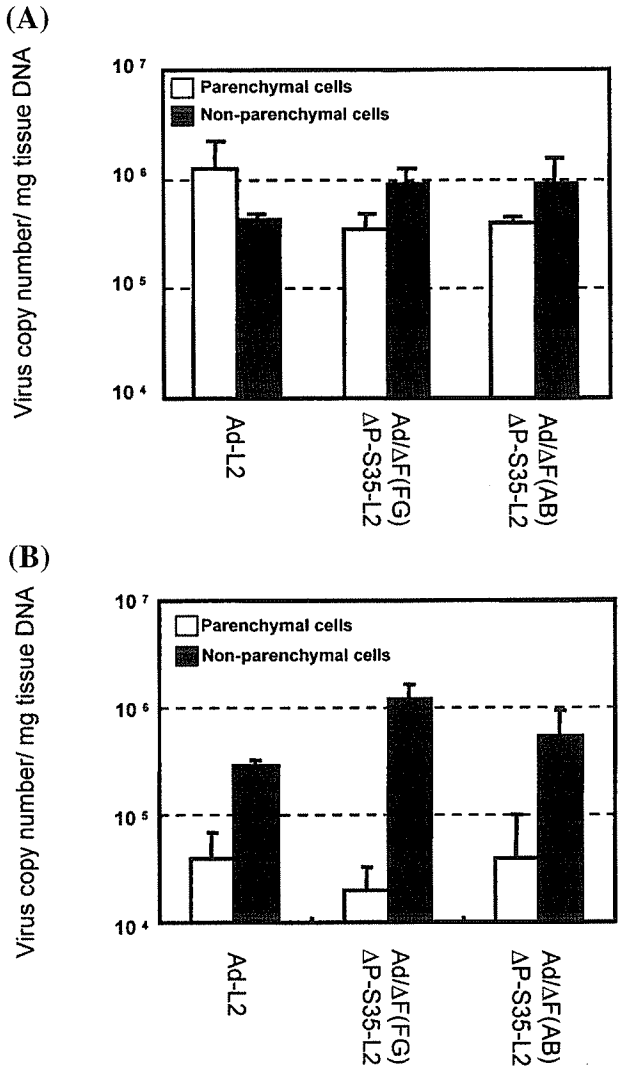

FIG. 5. Biodistribution of viral DNA in liver parenchymal and nonparenchymal cells. Ad-L2, Ad/ΔF(FG)ΔP-S35-L2, or Ad/ΔF(AB)ΔP-S35-L2 was (**A**) intravenously (3.0×10^{10} VP) or (**B**) intraperitoneally (1.0×10^{11} VP) injected into mice. Collagenase perfusion was performed 3 hr after injection of Ad vector to separate liver PCs and NPCs. Total DNA, including Ad vector DNA, was isolated from the cells, and Ad vector DNA was measured by quantitative TaqMan PCR assay. All data represent the means ± SD of four to six mice.

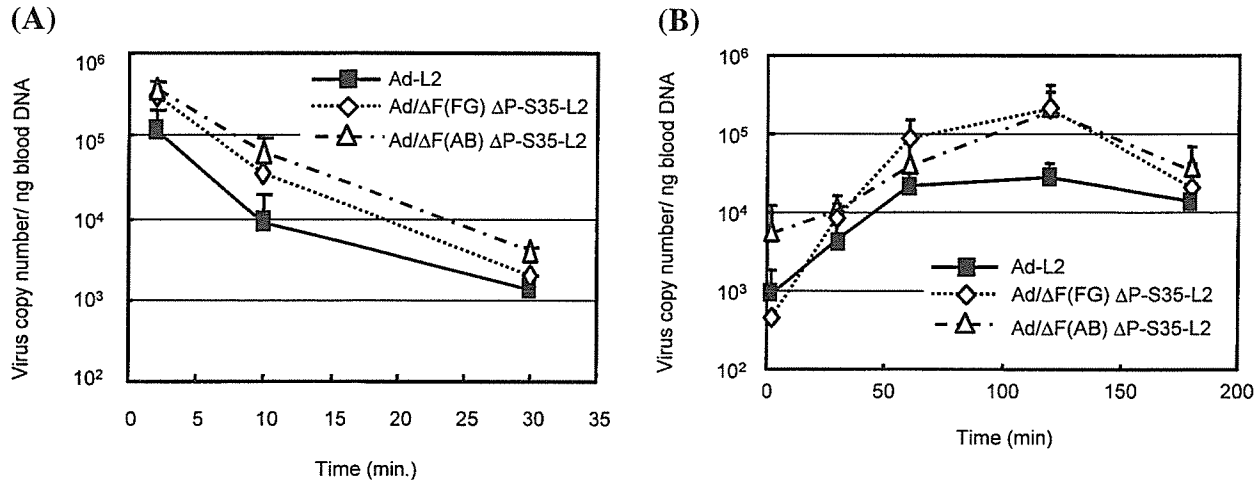

FIG. 6. Blood clearance of Ad-L2, Ad/ΔF(FG)ΔP-S35-L2, and Ad/ΔF(AB)ΔP-S35-L2 after systemic administration into mice. Ad-L2, Ad/ΔF(FG)ΔP-S35-L2, or Ad/ΔF(AB)ΔP-S35-L2 was (**A**) intravenously (3.0×10^{10} VP) or (**B**) intraperitoneally (1.0×10^{11} VP) injected, and blood was drawn by retroorbital bleeding at the indicated times postinjection. Total DNA, including Ad vector DNA, was isolated from the blood, and Ad vector DNA was measured by quantitative TaqMan PCR assay. All data represent the means ± SD of four to six mice.

Inclusion of RGD ligand into the fiber knob in triple-mutant Ad vectors

For the development of a targeted Ad vector, addition of foreign ligands into a viral capsid that no longer infects cells is required. For this purpose, Ad/ΔF(AB)ΔP-S35-RGD-L2, in which the RGD peptide was introduced into the HI loop of the fiber knob of Ad/ΔF(AB)ΔP-S35-L2, was constructed, and gene transfer activity was measured in SK HEP-1 cells (Fig. 9A). Ad/ΔF(AB)ΔP-S35-RGD-L2 showed 100-fold higher luciferase production in SK HEP-1 cells than did Ad/ΔF(AB)ΔP-S35-L2 (Fig. 9A). In the inhibition experiment using RGD peptide, luciferase production in cells transduced with Ad/ΔF(AB)ΔP-S35-RGD-L2 was suppressed by RGD peptide in a dose-dependent fashion, suggesting that Ad/ΔF(AB)ΔP-S35-RGD-L2 mediates gene transfer through RGD peptides in the fiber knob (Fig. 9B).

Next, to examine whether Ad/ΔF(AB)ΔP-S35-RGD-L2 mediates luciferase production *in vivo* in a manner different from Ad/ΔF(AB)ΔP-S35-L2, Ad/ΔF(AB)ΔP-S35-RGD-L2 was administered to mice by either intravenous (3.0×10^{10} VP) or intraperitoneal (1.0×10^{11} VP) injection, and luciferase production in organs was measured (Fig. 3). Data suggest that addition of RGD peptide to the triple-mutant Ad vector does not change the biodistribution *in vivo*, although intraperitoneal injection of Ad/ΔF(AB)ΔP-S35-RGD-L2 mediated slightly higher luciferase production in the spleen compared with Ad/ΔF(AB)ΔP-S35-L2.

DISCUSSION

In this study, we generated a new Ad vector with a four-amino acid mutation of the AB loop in the fiber knob (T489, A490, Y491, and T492), deletion of the RGD motif of the penton base, and substitution of the fiber shaft domain for that derived from Ad type 35, and demonstrated that this triple-mutant Ad vector shows significantly lower gene transfer activity (both *in vitro* and *in vivo*). The triple-mutant Ad vector containing a mutation of the AB loop in the fiber knob mediated much lower gene transfer activity than the previously generated triple-mutant Ad vector containing a mutation of the FG loop in the fiber knob (Koizumi *et al.*, 2003a). Furthermore, the triple-mutant Ad vector was less toxic, and showed almost background levels of both liver serum enzymes (AST and ALT) and IL-6 in mouse serum.

Ad vectors show nonspecific tissue distribution after *in vivo* gene transfer. This distribution is due largely to the relatively broad expression of CAR, α_v integrin, and HSGs; the size of sinusoidal fenestrae (Fechner *et al.*, 1999; Lievens *et al.*, 2004); and the complement system (Zinn *et al.*, 2004). To generate targeted Ad vectors, several groups have reported CAR binding-ablated Ad vectors with an AB or FG loop mutation of the fiber knob (Bewley *et al.*, 1999; Kirby *et al.*, 1999; Asaoka *et al.*, 2000; Alemany and Curiel, 2001; Einfeld *et al.*, 2001; Leissner *et al.*, 2001; Mizuguchi *et al.*, 2002; Smith *et al.*, 2002). However, there has been no report on the difference in gene transfer activity (*in vitro* and *in vivo*) between Ad vectors with an AB loop mutation and those with an FG loop mutation. The present study shows that mutation of the AB loop in the fiber knob is better than deletion of the FG loop for lowering transgene expression, at least with the triple-mutant Ad vector. Cells transduced with Ad/ΔF(AB)ΔP-S35-L2 or Ad/ΔF(FG)ΔP-S35-L2 produced luciferase at rates of only 0.003 and 0.42%, respectively, relative to the rate of luciferase production in cells transduced with Ad-L2 (Fig. 2A). The FG loop mutation in the fiber knob might continue to facilitate a weak interaction between CAR and the fiber knob. One of the interesting findings is that the amounts of Ad/ΔF(AB)ΔP-S35-L2 DNA and Ad/ΔF(FG)ΔP-S35-L2 DNA in the cells were only 10-fold lower than those of Ad-L2 DNA, even after the cells were treated with trypsin–EDTA and DNase I (Fig. 2B). Therefore, the cells would take up considerable amounts of Ad/ΔF(AB)ΔP-S35-L2 and Ad/ΔF(FG)ΔP-S35-L2 nonspecifically, although neither vector mediated luciferase production.

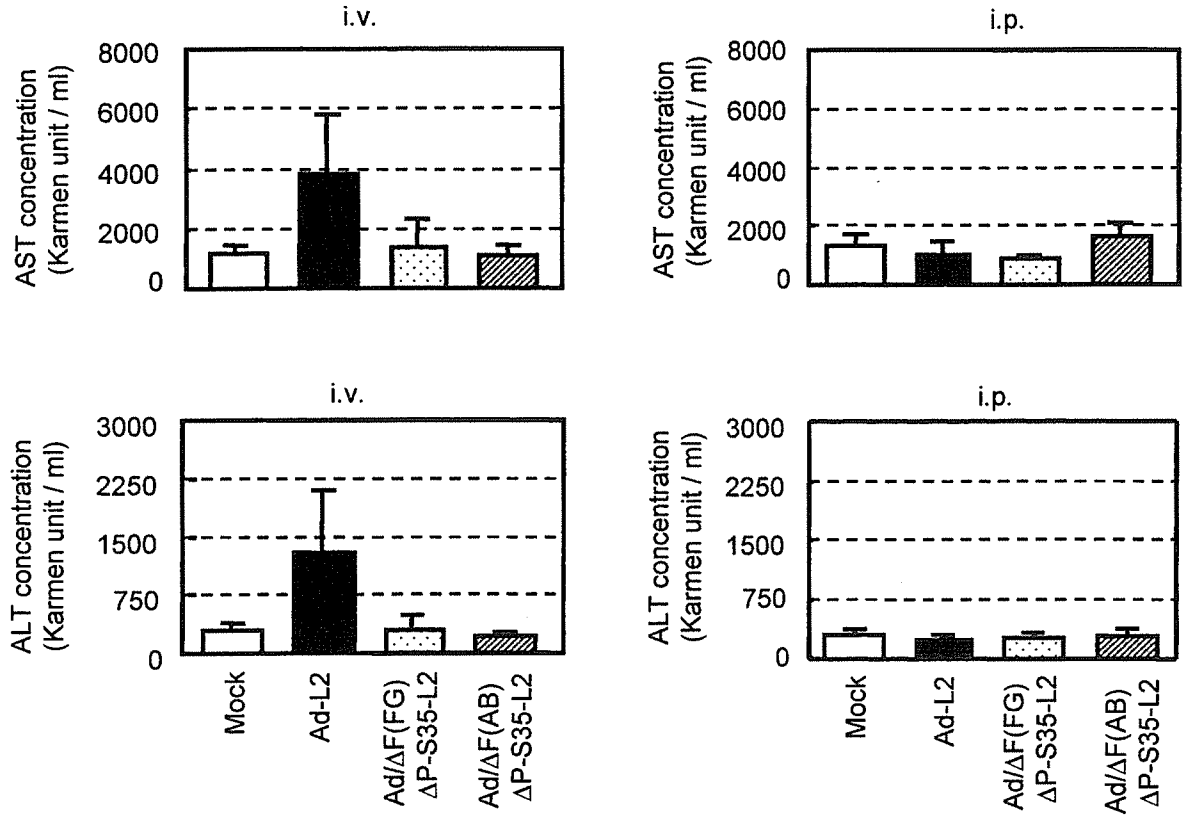

FIG. 7. Serum enzymes levels after systemic administration of Ad-L2, Ad/ΔF(FG)ΔP-S35-L2, or Ad/ΔF(AB)ΔP-S35-L2 into mice. Blood samples were collected from the inferior vena cava 48 hr after intravenous (3.0×10^{11} VP) or intraperitoneal (1.0×10^{11} VP) injection of Ad-L2, Ad/ΔF(FG)ΔP-S35-L2, or Ad/ΔF(AB)ΔP-S35-L2. Serum samples were collected into separate tubes containing no anticoagulant for coagulation, and aspartate aminotransferase (AST) and alanine aminotransferase (ALT) levels in serum were measured with a Transaminase-CII kit. All data represent the means ± SD of four mice.

We demonstrated that the newer triple-mutant Ad vector containing a mutation of the AB loop mediates approximately 15,000- and 500-fold lower mouse liver transduction by intravenous and intraperitoneal injection, respectively, than the conventional Ad vector (Fig. 3). However, the amounts of triple-mutant Ad vector DNA in the liver after intravenous or intraperitoneal injection were similar to or higher than those with the conventional Ad vector (Fig. 4). The difference between luciferase production and Ad DNA accumulation in the liver would be due to higher accumulation of triple-mutant Ad vector DNA in the NPCs (Kupffer cells and endothelial cells) (Fig. 5) as well as to nonspecific viral uptake in the liver. Because higher amounts of the triple-mutant Ad vector were taken up nonspecifically into the cultured cells (Fig. 2B), the liver cells *in vivo* would also take up large amounts of virus nonspecifically. Our previous report showed that most Ad DNA (especially the triple-mutant Ad DNA) taken up in NPCs disappears 48 hr after intravenous administration (Koizumi *et al.*, 2003a). Triple-mutant Ad vectors in NPCs might be resolved, resulting in significantly lower gene expression in the liver. Furthermore, Miyazawa *et al.* have reported that exchanging the Ad type 5 fiber (subgroup C) for the Ad type 7 fiber (subgroup B) on an Ad type 5 capsid resulted in altered cellular trafficking compared with parental Ad type 5 (Miyazawa *et al.*, 1999, 2001). Therefore, even if the triple-mutant Ad vector, in which the Ad type 5 fiber shaft was exchanged for the Ad type 35 fiber shaft (subgroup B), was taken up into cells, it might have defects in viral escape from the endosome to the cytoplasm (Nicklin *et al.*, 2005).

We and others have reported that the conventional Ad vector has a half-life in the bloodstream of approximately 2 min after intravenous injection (Alemany *et al.*, 2000; Alemany and Curiel, 2001; Koizumi *et al.*, 2003a; Sakurai *et al.*, 2003). The triple-mutant Ad vector and the conventional Ad vector presented similar clearance kinetics from the circulation after intravenous injection (Fig. 6A). In the case of intraperitoneal injection, the AUC_{2-180} value of the triple-mutant Ad vector in the bloodstream was approximately five to seven times higher than that of the conventional Ad vector (Fig. 6B). It remains unclear why intraperitoneally injected vectors persist longer in the blood (Akiyama *et al.*, 2004). The vector might associate with blood factors or cells (Shayakhmetov *et al.*, 2005). It was also found that intraperitoneally injected vectors accumulated more in NPCs than in PCs (Fig. 5B). This NPC-mediated uptake might be an obstacle for the targeted Ad vector when it is intraperitoneally injected. Because the present vector has no targeted ligands, more detailed studies should be done after high-affinity ligands are displayed on the vectors. If high levels of NPC-mediated uptake were avoided by the addition of ligands,

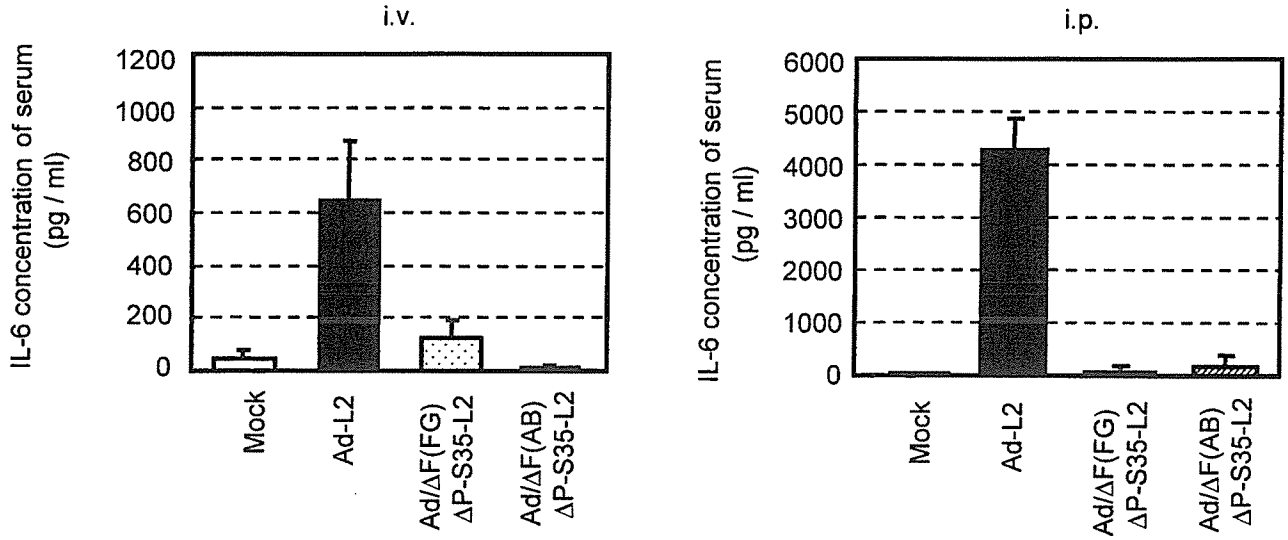

FIG. 8. Interleukin (IL)-6 levels in serum after systemic administration of Ad-L2, Ad/ΔF(FG)ΔP-S35-L2, or Ad/ΔF(AB)ΔP-S35-L2 into mice. Blood samples were collected from the inferior vena cava 3 hr after intravenous (3.0×10^{11} VP) or intraperitoneal (1.0×10^{11} VP) injection of Ad-L2, Ad/ΔF(FG)ΔP-S35-L2, or Ad/ΔF(AB)ΔP-S35-L2. Serum samples were collected into separate tubes containing no anticoagulant for coagulation, and IL-6 levels in the serum were measured by ELISA. All data represent the means ± SD of six mice.

the increased persistence of the vector in the blood in the case of intraperitoneal injection might give us a way to overcome obstacles to the development of targeted Ad vectors.

In the *in vivo* viral uptake experiment, the yield of viral DNA from total liver (Fig. 4) was an order of magnitude more than the total yield obtained from PCs and NPCs (Fig. 5). We speculated that extracellular virus, which would be present in the yield obtained from total liver but not in the yield obtained from fractionated cells, might be involved, because extracellular virus would be moved by collagenase treatment into the fractionated cells. To demonstrate this, we examined the effect of collagenase or trypsin treatment on the amounts of viral DNA in cultured cells. SK HEP-1 cells were transduced with Ad-L2 or Ad/ΔF(AB)ΔP-S35-L2 (3000 VP/cell). After a 3-hr culture period, the cells were washed with PBS, collagenase (0.01%), or trypsin (0.025%). The amounts of Ad genomic DNA in cells were

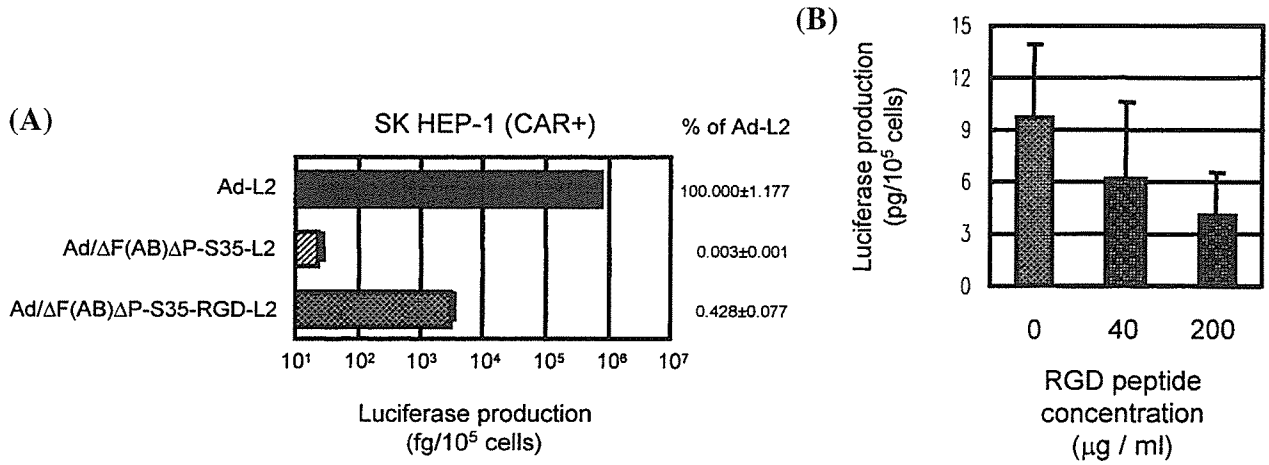

FIG. 9. Luciferase production in human cells transduced with Ad vectors containing RGD motif in the fiber knob. (**A**) Comparison of luciferase production in human cells transduced with Ad-L2, Ad/ΔF(AB)ΔP-S35-L2, or Ad/ΔF(AB)ΔP-S35-RGD-L2. SK HEP-1 cells were transduced with 3000 VP/cell of Ad-L2, Ad/ΔF(AB)ΔP-S35-L2, or Ad/ΔF(AB)ΔP-S35-RGD-L2 for 1.5 hr. After culture for 48 hr, luciferase production in the cells was measured by a luciferase assay system. The data are expressed as means ± SD ($n = 4$). The relative expression levels are described by designating the value of Ad-L2 as 100. (**B**) Effects of RGD peptide on the transduction efficiency of Ad/ΔF(AB)ΔP-S35-RGD-L2 into SK HEP-1 cells. SK HEP-1 cells were preincubated with RGD peptide (0, 1.6, 8, or 40 μg/ml) for 10 min. The cells were then transduced with 300 VP/cell of Ad/ΔF(AB)ΔP-S35-RGD-L2 for 0.5 hr in the presence of RGD peptide. After culture for 48 hr, luciferase production was measured by a luciferase assay system. The data are expressed as means ± SD ($n = 6$).

quantified with the TaqMan fluorogenic detection system. Data showed that collagenase or trypsin treatment decreased 2- to 3.5-fold the amounts of Ad DNA in cells (data not shown), suggesting that nonspecific viral association would lead to the overestimation of viral uptake by the cells. Therefore, the difference in the yields between Figs. 4 and 5 would be reasonable.

The initiation of inflammation and strong innate immunity responses occur after systemic administration of Ad vectors to animals and humans, and this toxicity limits the utility of Ad vectors for gene therapy (Muruve, 2004). Increased cytokine production after injection of Ad vectors was reported to be due to the introduction of input Ad vectors to Kupffer cells in the liver and dendritic cells (Lieber *et al.*, 1997; Schnell *et al.*, 2001; Morral *et al.*, 2002; Reid *et al.*, 2002; Philpott *et al.*, 2004). Lieber *et al.* have reported that IL-6 production in mice after injection of Ad vectors was decreased by preinjection of $GaCl_2$, which can decrease the levels of Kupffer cells in mouse liver (Lieber *et al.*, 1997). On the other hand, Muruve reported that Kupffer cells avidly take up systemically administered Ad vectors, but the blockade of Kupffer cells has minimal impact on the innate immune response in the liver (Muruve, 2004). Although our experiment showed that large amounts of the triple-mutant Ad vector accumulated in the NPC fraction, which contains Kupffer cells and liver sinusoidal (endothelial) cells, IL-6 was not produced in mice after injection of the triple-mutant Ad vector (Fig. 8). Therefore, Ad vectors would be capable of inducing IL-6 production in cells other than Kupffer cells. De Geest *et al.* reported that the spleen, not the liver, is the major site of IL-6 production after Ad vector transfer (De Geest *et al.* 2005), although in the present study the triple-mutant Ad vector accumulated in the spleen as much as did the conventional Ad vector (Fig. 4). There are several possible reasons why the triple-mutant Ad vector does not mediate IL-6 production *in vivo*. Philpott *et al.* have reported that maturation of dendritic cells, which are IL-6-producing cells, by infection with Ad vectors requires the RGD motif of the Ad penton base (Philpott *et al.*, 2004). The triple-mutant Ad vector without the RGD motif in the penton base would interact differently with IL-6-producing cells than would the conventional Ad vector. Liu *et al.* have reported that conventional Ad vectors are delivered into liver sinusoid cells as well as Kupffer cells after systemic injection (Liu *et al.*, 2003). Schiedner *et al.* have reported that Ad vectors activate liver endothelial cells after infection of Kupffer cells (Schiedner *et al.*, 2003). The difference in distribution between the triple-mutant Ad vector and the conventional Ad vector in liver sinusoid and Kupffer cells may contribute to IL-6 production. Furthermore, Zsengeller *et al.* demonstrated that Ad vector internalization and endosomal escape were required for cytokine induction in alveolar macrophages (Zsengeller *et al.*, 2000). The triple-mutant Ad vector might have reduced the level of endosomal escape in comparison with the conventional Ad vector. Specific viral component(s) of the Ad vector, viral distribution in the specific cell types, and/or viral distribution in the cellular compartment might determine IL-6 production. Elucidation of a mechanism for innate immune responses after administration of Ad vectors might be obtained by investigating the precise distribution of the triple-mutant Ad vector after systemic administration.

Finally, regarding the feasibility of using triple-mutant Ad vectors as targeted vectors, we constructed triple-mutant Ad vectors containing the RGD motif, which has high affinity for α_V integrins, in the HI loop of the fiber knob. This triple-mutant Ad vector with the RGD motif was found to show efficient *in vitro* gene transfer through RGD peptides in the fiber knob (Fig. 9). We also examined *in vivo* luciferase production and serum levels of AST, ALT, and IL-6 in mice after administration of this RGD motif-containing vector. However, the patterns of luciferase production *in vivo* (Fig. 3) and the serum levels of AST, ALT, and IL-6 (data not shown) postadministration were similar to those produced with the triple-mutant Ad vector without any ligands. Because the RGD peptide used in the present study was first isolated from a phage display library and used to "home" to endothelial cells in tumor tissue (Koivunen *et al.*, 1995; Pasqualini *et al.*, 1997), and because the endothelial cells in normal tissue do not express higher levels of α_V integrin than are found in tumor tissue, the RGD motif may not be the optimal peptide for increasing *in vivo* transduction efficiency after systemic injection. Another possible reason why this RGD motif-containing vector did not increase transduction *in vivo* is that the affinity of the introduced RGD peptides for integrin might be weak compared with the knob–CAR interaction. Furthermore, fiber mutation might affect encapsidation, stability, and flexibility of the vector. The resultant subtle alteration in fiber biology might negatively affect the transduction efficiency of this vector. Altered fiber biology might also be involved in the lower gene transduction efficiency of the triple-mutant Ad vector.

For the development of targeted Ad vectors, incorporation of a foreign ligand (i.e., peptide), one with high affinity for a specific cellular receptor, into the capsids of Ad vectors will also be required. The triple-mutant Ad vector was designed to have unique restriction sites (*Csp*45I or *Cla*I) in both the HI loop and the C-terminal coding region of the fiber knob (Mizuguchi *et al.*, 2001; Koizumi *et al.*, 2001, 2003b). Therefore, any targeting ligand can be easily displayed in the fiber knob of the triple-mutant Ad vector by cloning its gene into either of these regions, using simple *in vitro* ligation.

In summary, we have further improved the triple-mutant Ad vector by ablating CAR, α_V integrin, and HSG binding by introducing a mutation of the AB loop into the fiber knob (R412S, A415G, E416G, and K417G). This vector was found to mediate significantly lower tissue transduction both *in vitro* and *in vivo* (intravenous and intraperitoneal injection). Furthermore, we showed that this triple-mutant Ad vector reduces (or blunts) liver toxicity and innate immunity responses (IL-6 production). Inclusion of the RGD peptide in the HI loop of the fiber knob of the triple-mutant Ad vector restored gene transfer activity. Thus, the newer triple-mutant Ad vector will likely be a fundamental vector for targeted gene delivery.

ACKNOWLEDGMENTS

The authors thank Tomomi Sasaki and Takashi Fukushima for technical assistance. This work was supported by grants from the Ministry of Health, Labor, and Welfare of Japan and a Grant-in-Aid for Scientific Research in Priority Areas from the Ministry of Education, Culture, Sports, Science, and Technology (MEXT) of Japan. T.H. is the recipient of a fellowship from the Japan Society for the Promotion of Science.

REFERENCES

AKIYAMA, M., THORNE, S., KIRN, D., ROELVINK, P., EINFELD, D., KING, C., and WICKHAM, T. (2004). Ablating CAR and integrin binding in adenovirus vectors reduces nontarget organ transduction and permits sustained bloodstream persistence following intraperitoneal administration. Mol. Ther. **9,** 218–230.

ALEMANY, R., and CURIEL, D.T. (2001). CAR-binding ablation does not change biodistribution and toxicity of adenoviral vectors. Gene Ther. **8,** 1347–1353.

ALEMANY, R., SUZUKI, K., and CURIEL, D.T. (2000). Blood clearance rates of adenovirus type 5 in mice. J. Gen. Virol. **81,** 2605–2609.

ASAOKA, K., TADA, M., SAWAMURA, Y., IKEDA, J., and ABE, H. (2000). Dependence of efficient adenoviral gene delivery in malignant glioma cells on the expression levels of the coxsackievirus and adenovirus receptor. J. Neurosurg. **92,** 1002–1008.

BERGELSON, J.M., CUNNINGHAM, J.A., DROGUETT, G., KURT-JONES, E.A., KRITHIVAS, A., HONG, J.S., HORWITZ, M.S., CROWELL, R.L., and FINBERG, R.W. (1997). Isolation of a common receptor for coxsackie B viruses and adenoviruses 2 and 5. Science **275,** 1320–1323.

BEWLEY, M.C., SPRINGER, K., ZHANG, Y.B., FREIMUTH, P., and FLANAGAN, J.M. (1999). Structural analysis of the mechanism of adenovirus binding to its human cellular receptor, CAR. Science **286,** 1579–1583.

DE GEEST, B., SNOEYS, J., VAN LINTHOUT, S., LIEVENS, J., and COLLEN, D. (2005). Elimination of innate immune responses and liver inflammation by PEGylation of adenoviral vectors and methylprednisolone. Hum. Gene Ther. **16,** 1439–1451.

EINFELD, D.A., SCHROEDER, R., ROELVINK, P.W., LIZONOVA, A., KING, C.R., KOVESDI, I., and WICKHAM, T.J. (2001). Reducing the native tropism of adenovirus vectors requires removal of both CAR and integrin interactions. J. Virol. **75,** 11284–11291.

FECHNER, H., HAACK, A., WANG, H., WANG, X., EIZEMA, K., PAUSCHINGER, M., SCHOEMAKER, R., VEGHEL, R., HOUTSMULLER, A., SCHULTHEISS, H.P., LAMERS, J., and POLLER, W. (1999). Expression of coxsackie adenovirus receptor and α_v-integrin does not correlate with adenovector targeting *in vivo* indicating anatomical vector barriers. Gene Ther. **6,** 1520–1535.

HEFFELFINGER, S.C., HAWKINS, H.H., BARRISH, J., TAYLOR, L., and DARLINGTON, G.J. (1992). SK HEP-1: A human cell line of endothelial origin. In Vitro Cell Dev. Biol. **28A,** 136–142.

HONG, S., MAGNUSSON, M., HENNING, P., LINDHOLM, L., and BOULANGER, P. (2003). Adenovirus stripping: A versatile method to generate adenovirus vectors with new cell target specificity. Mol. Ther. **1,** 692–699.

KIRBY, I., DAVISON, E., BEAVIL, A., SOH, C., WICKHAM, T., ROELVINK, P., KOVESDI, I., SUTTON, B., and SANTIS, G. (1999). Mutations in the DG loop of adenovirus type 5 fiber knob protein abolish high-affinity binding to its cellular receptor CAR. J. Virol. **11,** 9508–9514.

KOIVUNEN, E., WANG, B., and RUOSLAHTI, E. (1995). Phage libraries displaying cyclic peptides with different ring sizes: Ligand specificities of the RGD-directed integrins. Biotechnology **13,** 265–270.

KOIZUMI, N., MIZUGUCHI, H., HOSONO, T., ISHII-WATABE, A., UCHIDA, E., UTOGUCHI, N., WATANABE, Y., and HAYAKAWA, T. (2001). Efficient gene transfer by fiber-mutant adenoviral vectors containing RGD peptide. Biochim. Biophys. Acta **1568,** 13–20.

KOIZUMI, N., MIZUGUCHI, H., SAKURAI, F., YAMAGUCHI, T., WATANABE, Y., and HAYAKAWA, T. (2003a). Reduction of natural adenovirus tropism to mouse liver by fiber-shaft exchange in combination with both CAR- and α_v integrin-binding ablation. J. Virol. **77,** 13062–13072.

KOIZUMI, N., MIZUGUCHI, H., UTOGUCHI, N., WATANABE, Y., and HAYAKAWA, T. (2003b). Generation of fiber-modified adenovirus vectors containing heterologous peptides in both the HI loop and C terminus of the fiber knob. J. Gene Med. **5,** 267–276.

KRASNYKH, V., DOUGLAS, J., and VAN BEUSECHEM, W. (2000). Genetic targeting of adenoviral vectors. Mol. Ther. **1,** 391–405.

LEISSNER, P., LEGRAND, V., SCHLESINGER, Y., HADJI, D.A., VAN RAAIJ, M., CUSACK, S., PAVIRANI, A., and MEHTALI, M. (2001). Influence of adenoviral fiber mutations on viral encapsidation, infectivity and *in vivo* tropism. Gene Ther. **8,** 49–57.

LIEBER, A., HE, C., MEUSE, L., SCHOWALTER, D., KIRILLOVA, I., WINTHER, B., and KAY, M. (1997). The role of Kupffer cell activation and viral gene expression in early liver toxicity after infusion of recombinant adenovirus vectors. J. Virol. **71,** 8798–8807.

LIEVENS, J., SNOEYS, J., VEKEMANS, K., VAN LINTHOUT, S., DE ZANGER, R., COLLEN, D., WISSE, E., and DE GEEST, B. (2004). The size of sinusoidal fenestrae is a critical determinant of hepatocyte transduction after adenoviral gene transfer. Gene Ther. **11,** 1523–1531.

LIU, Q., ZAISS, A., COLARUSSO, P., PATEL, K., HALJAN, G., WICKHAM, T., and MURUVE, D. (2003). The role of capsid–endothelial interactions in the innate immune response to adenovirus vectors. Hum. Gene Ther. **14,** 627–643.

MAIZEL, J.V.J., WHITE, D.O., and SCHARFF, M.D. (1968). The polypeptides of adenovirus. I. Evidence for multiple protein components in the virion and a comparison of types 2, 7A, and 12. Virology **36,** 115–125.

MIYAZAWA, N., CRYSTAL, R., and LEOPOLD, P. (1999). Adenovirus serotype 7 retention in a late endosomal compartment prior to cytosol escape is modulated by fiber protein. J. Virol. **75,** 1387–1400.

MIYAZAWA, N., LEOPOLD, P., HACKETT, N., FERRIS, B., WORGALL, S., FALCK-PEDERSEN, E., and CRYSTAL, R. (2001). Fiber swap between adenovirus subgroups B and C alters intracellular trafficking of adenovirus gene transfer vectors. J. Virol. **73,** 6056–6065.

MIZUGUCHI, H., and HAYAKAWA, T. (2002). Adenovirus vectors containing chimeric type 5 and type 35 fiber proteins exhibit altered and expanded tropism and increase the size limit of foreign genes. Gene **285,** 69–77.

MIZUGUCHI, H., and HAYAKAWA, T. (2004). Targeted adenovirus vectors. Hum. Gene Ther. **15,** 1034–1044.

MIZUGUCHI, H., and KAY, M.A. (1998). Efficient construction of a recombinant adenovirus vector by an improved *in vitro* ligation method. Hum. Gene Ther. **9,** 2577–2583.

MIZUGUCHI, H., and KAY, M.A. (1999). A simple method for constructing E1 and E1/E4 deleted recombinant adenovirus vector. Hum. Gene Ther. **10,** 2013-2017.

MIZUGUCHI, H., KOIZUMI, N., HOSONO, T., UTOGUCHI, N., WATANABE, Y., KAY, M.A., and HAYAKAWA, T. (2001). A simplified system for constructing recombinant adenoviral vectors containing heterologous peptides in the HI loop of their fiber knob. Gene Ther. **8,** 730–735.

MIZUGUCHI, H., KOIZUMI, N., HOSONO, T., ISHII-WATABE, A., UCHIDA, E., UTOGUCHI, N., WATANABE, Y., and HAYAKAWA, T. (2002). CAR- or α_v integrin-binding ablated adenovirus vectors, but not fiber-modified vectors containing RGD peptide, do not change the systemic gene transfer properties in mice. Gene Ther. **9,** 769–776.

MORRAL, N., O'NEAL, W., RICE, K., LELAND, M., PIEDRA, P., AGUILAR-CORDOVA, E., CAREY, K., BEAUDET, A., and LANGSTON, C. (2002). Lethal toxicity, severe endothelial injury, and a threshold effect with high doses of an adenoviral vector in baboons. Hum. Gene Ther. **13,** 143–154.

MURUVE, D. (2004). The innate immune response to adenovirus vectors. Hum. Gene Ther. **15,** 1157–1166.

NAKAMURA, T., SATO, K., and HAMADA, H. (2003). Reduction of natural adenovirus tropism to the liver by both ablation of

fiber–coxsackievirus and adenovirus receptor interaction and use of replaceable short fiber. J. Virol. **77,** 2512–2521.

NICKLIN, S., WU, E., NEMEROW, G., and BAKER, A. (2005). The influence of adenovirus fiber structure and function on vector development for gene therapy. Mol. Ther. **12,** 384–393.

NISHIKAWA, M., TAKEMURA, S., TAKAKURA, Y., and HASHIDA, M. (1998). Targeted delivery of plasmid DNA to hepatocytes *in vivo*: Optimization of the pharmacokinetics of plasmid DNA/galactosylated poly(L-lysine) complexes by controlling their physicochemical properties. J. Pharmacol. Exp. Ther. **287,** 408–415.

PASQUALINI, R., KOIVUNEN, E., and RUOSLAHTI, E. (1997). α_v integrins as receptors for tumor targeting by circulating ligands. Nat. Biotechnol. **15,** 542–546.

PHILPOTT, N., NOCIARI, M., ELKON, K., and FALCK-PEDERSEN, E. (2004). Adenovirus-induced maturation of dendritic cells through a PI3 kinase-mediated TNF-α induction pathway. Proc. Natl. Acad. Sci. U.S.A. **101,** 6200–6205.

REID, T., GALANIS, E., ABBRUZZESE, J., SZE, D., WEIN, L., ANDREWS, J., RANDLEV, B., HEISE, C., UPRICHARD, M., HATFIELD, M., ROME, L., RUBIN, J., and KIRN, D. (2002). Hepatic arterial infusion of a replication-selective oncolytic adenovirus (dl1520): Phase II viral, immunologic, and clinical endpoints. Cancer Res. **62,** 6070–6079.

SAKURAI, F., MIZUGUCHI, H., YAMAGUCHI, T., and HAYAKAWA, T. (2003). Characterization of *in vitro* and *in vivo* gene transfer properties of adenovirus serotype 35 vector. Mol. Ther. **8,** 813–821.

SCHIEDNER, G., BLOCH, W., HERTEL, S., JOHNSTON, M., MOLOJAVYI, A., DRIES, V., VARGA, G., VAN ROOIJEN, N., and KOCHANEK, S. (2003). A hemodynamic response to intravenous adenovirus vector particles is caused by systemic Kupffer cell-mediated activation of endothelial cells. Hum. Gene Ther. **14,** 1631–1641.

SCHNELL, M., ZHANG, Y., TAZELAAR, J., GAO, G., YU, Q., QIAN, R., CHEN, S., VARNAVSKI, A., LECLAIR, C., RAPER, S., and WILSON, J. (2001). Activation of innate immunity in nonhuman primates following intraportal administration of adenoviral vectors. Mol. Ther. **3,** 708–722.

SHAYAKHMETOV, D., GAGGAR, A., NI, S., LI, Z., and LIEBER, A. (2005). Adenovirus binding to blood factors results in liver cell infection and hepatotoxicity. J. Virol. **72,** 7478–7491.

SMITH, T., IDAMAKANTI, N., KYLEFJORD, H., ROLLENCE, M., KING, L., KALOSS, M., KALEKO, M., and STEVENSON, S.C. (2002). *In vivo* hepatic adenoviral gene delivery occurs independently of the coxsackievirus–adenovirus receptor. Mol. Ther. **5,** 770–779.

SMITH, T., IDAMAKANTI, N., ROLLENCE, M.L., MARSHALL-NEFF, J., KIM, J., MULGREW, K., NEMEROW, G.R., KALEKO, M., and STEVENSON, S.C. (2003a). Adenovirus serotype 5 fiber shaft influences *in vivo* gene transfer in mice. Hum. Gene Ther. **14,** 777–787.

SMITH, T., IDAMAKANTI, N., MARSHALL-NEFF, J., ROLLENCE, M., WRIGHT, P., KALOSS, M., KING, L., MECH, C., DINGES, L., IVERSON, W., SHERER, A., MARKOVITS, J., LYONS, R., KALEKO, M., and STEVENSON, S. (2003b). Receptor interactions involved in adenoviral-mediated gene delivery after systemic administration in non-human primates. Hum. Gene Ther. **14,** 1595–1604.

TOMKO, R.P., XU, R., and PHILIPSON, L. (1997). HCAR and MCAR: The human and mouse cellular receptors for subgroup C adenoviruses and group B coxsackieviruses. Proc. Natl. Acad. Sci. U.S.A. **94,** 3352–3356.

VIGNE, E., DEDIEU, J., BRIE, A., GILLARDEAUX, A., BRIOT, D., BENIHOUD, K., LATTA-MAHIEU, M., SAULNIER, P., PERRICAUDET, M., and YEH, P. (2003). Genetic manipulations of adenovirus type 5 fiber resulting in liver tropism attenuation. Gene Ther. **10,** 153–162.

WICKHAM, T.J. (2000). Targeting adenovirus. Gene Ther. **7,** 110–114.

WICKHAM, T.J., MATHIAS, P., CHERESH, D.A., and NEMEROW, G.R. (1993). Integrins $\alpha_v\beta_3$ and $\alpha_v\beta_5$ promote adenovirus internalization but not virus attachment. Cell **73,** 309–319.

WICKHAM, T.J., FILARDO, E.J., CHERESH, D.A., and NEMEROW, G.R. (1994). Integrin $\alpha_v\beta_5$ selectively promotes adenovirus mediated cell membrane permeabilization. J. Cell Biol. **127,** 257–264.

XU, Z.-L., MIZUGUCHI, H., ISHII-WATABE, A., UCHIDA, E., MAYUMI, T., and HAYAKAWA, T. (2001). Optimization of transcriptional regulatory elements for constructing plasmid vectors. Gene **272,** 149–156.

ZINN, K., SZALAI, A., STARGEL, A., KRASNYKH, V., and CHAUDHURI, T. (2004). Bioluminescence imaging reveals a significant role for complement in liver transduction following intravenous delivery of adenovirus. Gene Ther. **11,** 1482–1486.

ZSENGELLER, Z., OTAKE, K., HOSSAIN, S.A., BERCLAZ, P.Y., and TRAPNELL, B.C. (2000). Internalization of adenovirus by alveolar macrophages initiates early proinflammatory signaling during acute respiratory tract infection. J. Virol. **74,** 9655–9667.

Address reprint requests to:
Dr. Hiroyuki Mizuguchi
National Institute of Biomedical Innovation
Asagi 7-6-8, Saito
Ibaraki, Osaka 567-0085, Japan

E-mail: mizuguch@nibio.go.jp

Received for publication August 3, 2005; accepted after revision December 9, 2005.

Published online: February 8, 2006.